Published in final edited form as:
J Pharmacol Exp Ther. 2008 September ; 326(3): 700–716. doi:10.1124/jpet.108.140186.

Circadian Variations in Liver Gene Expression: Relationships to Drug Actions

Richard R. Almon, **Eric Yang**, **William Lai**, **Ioannis P. Androulakis**, **Debra C. DuBois**, and **William J. Jusko**
Department of Biological Sciences, State University of New York at Buffalo, Buffalo, NY 14260 (RRA, WL, DCD)Department of Pharmaceutical Sciences, State University of New York at Buffalo, Buffalo, NY 14260 (RRA, DCD, WJJ)New York State Center of Excellence in Bioinformatics and Life Sciences (RRA, WJJ)Biomedical Engineering Department, Rutgers University Piscataway, NJ 08854 (EY, IA)

Abstract

Chronopharmacology is an important but under-explored aspect of therapeutics. Rhythmic variations in biological processes can influence drug action, including pharmacodynamic responses, due to circadian variations in the availability or functioning of drug targets. We hypothesized that global gene expression analysis can be useful in the identification of circadian regulated genes involved in drug action. Circadian variations in gene expression in rat liver were explored using Affymetrix gene arrays. A rich time series involving animals analyzed at 18 time points within the 24 hour cycle was generated. Of the more than 15,000 probe sets on these arrays, 265 exhibited oscillations with a 24 hour frequency. Cluster analysis yielded 5 distinct circadian clusters, with approximately two-thirds of the transcripts reaching maximum expression during the animal's dark/active period. Of the 265 probe sets, 107 of potential therapeutic importance were identified. The expression levels of clock genes were also investigated in this study. Five clock genes exhibited circadian variation in liver, and data suggest that these genes may also be regulated by corticosteroids.

INTRODUCTION

Virtually all organisms have biological rhythms associated with the light-dark cycle (Badiu, 2003; Oishi et al., 2003; Murphy, 2005; Ueda et al., 2005). In mammals, rhythms exist at all levels of organization from the organismal to the cellular. The central orchestrators of these rhythms are paired suprachiasmatic nuclei (SCN) in the anterior part of the hypothalamus which receive direct input by way of the retinohypothalamic tract. However, the existence of diurnal and nocturnal animals and the ability of animals to shift with changes in the light-dark cycle indicate that beyond the SCN the rhythms are not slaves to the presence or absence of light (Dardente et al., 2002; Challet et al., 2003). In addition to receiving inputs from the retina, the SCN also receives inputs from forebrain areas that modulate the downstream influences of the SCN. Of particular importance to rhythmicity in peripheral tissues are outputs from the SCN which are directed to other parts of the hypothalamus that regulate both anterior and posterior pituitary hormones, as well as the autonomic nervous system. In addition, behavioral adjuncts associated with the exigencies of life such as feeding and activity can impact rhythmicity downstream of the SCN.

Corresponding Author: Richard R. Almon, Department of Biological Sciences, 107 Hochstetter Hall, State University of New York at Buffalo, Buffalo, NY 14260, Phone: 716-645-2363 ext 113, FAX: 716-645-2975, email: almon@eng.buffalo.edu.

In the SCN the circadian clock involves an autoregulatory negative feedback loop of gene expression (Dardente et al., 2002; Challet et al., 2003; Ueda et al., 2005). Its basic elements are several transcription factors including CLOCK (Circadian Locomotor Output Cycles Kaput) and BMAL1 (Aryl Hydrocarbon Receptor Nuclear Translocator-like) which heterodimerize and enhance the expression of PERIOD (PER) and CRYPYOCHROME (CRY). In turn, PER and CRY heterodimerize and repress the expression of CLOCK and BMAL1. The core system is entrained to the light/dark cycle with CLOCK:BMAL being high during the light and PER:CRY being high during the dark (Ueda et al., 2005). In addition to the core transcription factors, there are additional transcription factors that add flexibility and adaptability to the central clock.

The central clock anticipates the change in photoperiods, preparing the animal for the upcoming period of activity and feeding, regardless of whether that period is in light or dark. The input from the SCN to the regulation of both pituitary hormones and the autonomic nervous system impart rhythmicity to peripheral tissues. However, this is further complicated by more diffuse behavior-related factors which alter systemic demands. Many of the transcription factors involved in regulating the central clock are also expressed in peripheral tissues. However, their regulation is complicated by variations in ancillary factors. The existence of both diurnal and nocturnal mammals and the phenomena of phase shifting by food restriction illustrate both the complexity and flexibility in peripheral rhythmicity. Its intrinsic nature is illustrated by the observations that rhythmic behavior with a periodicity of approximately 24 hours can be induced in a variety of cells in culture (Ueda et al., 2005).

The hypothalmic/pituitary/adrenal axis (HPA) is of particular importance to the active feeding period. Its effector hormones, glucocorticoids, are high during the light period in diurnal animals and during the dark period in nocturnal animals (Dardente et al., 2002). The mechanism for most glucocorticoid effects involves modulation in the amount of specific mRNAs (Almon et al., 2007). By virtue of their circadian periodicity, glucocorticoids are effectors of many circadian changes in gene expression.

The liver expresses an unusually large and diverse repertoire of genes (Almon et al., 2007). The nature of the processes carried out by liver suggests that many of its expressed genes should be under circadian control either directly or indirectly. In the present report we describe the use of Affymetrix arrays to analyze the livers of rats maintained on a strict light/dark regimen consisting of 12 hours light/12 hours dark with three animals sacrificed at 18 time points during the 24 hour period. This rich time series allowed us to group genes into five relatively discrete circadian clusters. Circadian responsive genes were also examined within the context of glucocorticoid regulation and their response to exogenous corticosteroids.

The probe sets that were found to have an oscillation with a 24 hour frequency had their identities confirmed when possible using the Basic Local Alignment and Search Tool (BLAST). This information was used to parse the genes into 13 functional groups. Functional groups were then analyzed by clusters to determine the distribution of these functions in circadian time.

Dysregulation of aspects of liver function are associated with a variety of common pathologies. As a result, liver functions are commonly targeted by drugs. It has been long recognized that rhythmic variations in biological processes can affect therapeutics, including absorption/distribution, excretion, protein binding, and response (Reinberg, 1992; Labrecque et al., 1995; Smolensky et al., 1999). Therefore the circadian regulation of gene expression was also examined and discussed within the context of drug targeting, with emphasis of cholesterol/bile acid synthesis, cancer chemotherapeutics, and translation and protein processing.

METHODS

Animals

Fifty-four normal (150–175 g) male Wistar rats were purchased in two separate batches of 27 from Harlan Sprague-Dawley Inc. (Indianapolis, IN, USA) and experiments were initiated at body weights between 225 and 275 g. Animals were housed and allowed to acclimatize in a constant-temperature environment (22°C) equipped with a 12-h light/dark cycle. Twenty-seven rats (Group I) were acclimatized for 2 weeks prior to study to a normal light/dark cycle, where lights went on at 8 AM and off at 8 PM. The onset of the light period was considered as time zero. The other 27 rats (Group II) were acclimatized for 2 weeks prior to study to a reversed light/dark cycle, where lights went on at 8 PM and off at 8 AM. Rats in Group I were killed on three successive days at 0.25, 1, 2, 4, 6, 8, 10, 11, and 11.75 hr after lights on to capture the light period. Rats in Group II were killed on three successive days at 12.25, 13, 14, 16, 18, 20, 22, 23, and 23.75 h after lights on to capture the dark period. Animals sacrificed at the same time on successive days were treated as triplicate measurements. Because normal rats were used, minimal animal handling with least possible environmental disturbances was employed to minimize stress. Night vision goggles were used to carry out animal procedures conducted in the dark period. At sacrifice, rats were weighed, anesthetized by ketamine/xylazine, and sacrificed by aortic exsanguination. Blood was drawn from the abdominal aortic artery into syringes using ethylenediaminetetraacetic acid (4mM final concentration) as anticoagulant. Plasma was harvested from blood by centrifugation (2000 × g, 15 minutes, 4° C) and frozen at minus 80°C until analyzed for corticosterone. Livers were excised and frozen in liquid nitrogen immediately after sacrifice and stored at minus 80°C until RNA preparation. Both acute and chronic MPL dosing experiments have been previously published (Almon et al., 2007). In brief, populations of adrenalectamized male Wistar rats were given doses of the synthetic glucocorticoid, methylprednisolone (MPL). In the acute experiment the animals were given a single bolus dose (50 mg/kg) of MPL and were sacrificed at 16 times over a 72 hour period following dosing. In the chronic experiment, the animals received a constant infusion of 0.3 mg/kg/h MPL via Alzet osmotic pumps and were sacrificed at 10 times over a 168 hour period. All rats had free access to rat chow and 0.9% saline drinking water. Our research protocol adheres to the Principles of Laboratory Animal Care (NIH publication 85-23, revised in 1985) and was approved by the University at Buffalo Institutional Animal Care and Use Committee.

Plasma Steroid Assays

Plasma corticosterone concentrations were determined by a sensitive normal-phase high-performance liquid chromatography (HPLC) method as previously described (Haughey and Jusko, 1988). The limit of quantitation was 10 ng/ml. The interday and intraday coefficients of variation (CV) were less than 10%.

Microarrays

Liver samples from each animal were ground into a fine powder in a mortar cooled by liquid nitrogen and 100 mg was added to 1 ml of pre-chilled Trizol Reagent (InVitrogen, Carlsbad CA). Total RNA extractions were carried out according to manufacturer's directions and were further purified by passage through RNeasy mini-columns (QIAGEN, Valencia, CA) according to manufacturer's protocols for RNA clean-up. Final RNA preparations were resuspended in RNase-free water and stored at −80°C. The RNAs were quantified spectrophotometrically, and purity and integrity assessed by agarose gel electrophoresis. All samples exhibited 260/280 absorbance ratios of approximately 2.0, and all showed intact ribosomal 28S and 18S RNA bands in an approximate ratio of 2:1 as visualized by ethidium bromide staining. Isolated RNAs from each liver sample was used to prepare the hybridization targets according to manufacturer's protocols. The biotinylated cRNAs were hybridized to 54

individual Affymetrix GeneChips Rat Genome 230A (Affymetrix, Inc., Santa Clara, CA), which contained 15,967 probe sets. The 230A chip was used in the chronic infusion experiment as well allowing direct comparison between the two experiments. The 230A gene chips contain over 7,000 more probe sets more than the ones used (U34A) in our earlier muscle bolus dose MPL study (Almon et al., 2005). The high reproducibility of in situ synthesis of oligonucleotide chips allows accurate comparison of signals generated by samples hybridized to separate arrays. This data set has been submitted to GEO (GSE8988).

Dataset construction

As detailed above, animals were sacrificed at precise times on three successive days to obtain data points for the light period and three successive days to obtain data points for the dark period. Animals sacrificed at the same time on different days were treated as three replicates for that time to construct a 24 hr light:dark cycle. In order to obtain a clear picture of an entire cycle, two 24 hr periods were concatenated to obtain a 48 hr period which allowed visualization of rhythms that spanned the dark/light and dark/light transitions.

Data mining

A non-linear curve fit using MATLAB was conducted which fitted a sinus function [A*sin(Bt + c)] to the data including the replicates. Genes that could be curve fitted with a R^2 correlation of greater than 0.8 were kept. This curve fitting approach enabled use of replicate information instead of depending on the ensemble average necessary with Fourier transforms or Lombs Scargle methods. This approach is viable due to our relatively large number of time samples. This dataset was then loaded into a data mining program, GeneSpring 7.0 (Silicon Genetics, Redwood City, CA), and we normalized the value of each probe set on each chip to the average of that probe set on all chips. In order to identify genes with similar patterns of oscillation within the daily cycle we applied Quality Threshold Clustering (QT) in GeneSpring using Pearson's correlation as the similarity measurement.

RESULTS

Data mining

It is assumed that genes whose expression levels are part of the circadian rhythm will show one full oscillation every twenty-four hours. However, in light of possible ultradian or infradian cycles within the data, we have utilized a much more general model of periodic signals given as [A*sin(Bt + c)]. A non-linear curve fit was conducted which fitted a sinusoid to the data including the replicates. We identified 265 probe sets which fit the model [A*sin(Bt + c)] with a R^2 correlation greater than 0.8. With this more general model, we found that all genes which showed a high level of correlation had similar values for B and showed one full cycle over 24 hours. This suggests that while there may exist ultradian or infradian signals, they were not evident in the experimental dataset, perhaps due to the sampling strategy employed in the experimental design. Using GeneSpring, we normalized the value of each probe set on each chip to the average of that probe set on all chips such that the expression pattern of all probe sets oscillated approximately around 1. There appear to be two major patterns as illustrated in Figure 1, with one pattern reflecting maximum expression during the light/inactive period while the others reach a maximum during the dark/active period. However, oscillations in expression have more discrete relationships to the light/dark periods. In order to group genes with similar patterns within the daily cycle we applied QT Clustering, yielding 5 clusters. Figure 2 shows these five clusters with the centriod (average of all of the genes in each cluster) highlighted in white. Approximately two-thirds of the probe sets reach maximum expression during the dark/active period. Supplementary Tables 1–5 (available online) provide a detailed list of all genes in each cluster, including Probe Set ID, Accession Number, Pearson's correlation coefficient with the centroid, gene symbol, gene name, and gene function.

Corticosterone reaches its maximum plasma concentration in these animals at hour 13.3 (Figure 3).

Regulation

Three basic categories of transcription factors have been associated with control of circadian oscillation in gene expression. The first are those that participate through E-Box binding, the second through DBP/E4BP4 binding elements (D-boxes), and the last through RevErbA/ROR binding elements (RREs). We examined the chip for probe sets for transcription factors previously identified as involved in regulation of circadian patterns (Ueda et al., 2005). The 230A chip contained probe sets for 16 out of 17 of these transcription factors. However, only five (PER2, BMAL1b, DBP, Nr1d1, and Nr1d2) showed distinct circadian oscillation. Figure 4 shows the circadian patterns of these five genes in relation to the light/inactive and dark/active periods. Consistent with the literature on the core clock in the SCN, BMAL1b reaches a maximum during the light period while PER2 reaches a maximum during the dark period. The chip did contain probe sets for Clock, PER1, PER 3, CRY2, Bhlhb2 (Basic Helix-Loop-Helix Domain-Containing Protein, Class B 2, Dec1); Bhlhb3 (Basic Helix-Loop-Helix Domain-Containing Protein, Class B 3, Dec2, Sharp1); NFIL3A (Nuclear Factor, Interleukin 3 Regulated, E4BP4); RORA (RAR-Related Orphan Receptor A, RAR-Related Orphan Receptor Alpha, RZR-Alpha, RZRA, Retinoic Acid-Binding Receptor Alpha); RORB (RAR-Related Orphan Receptor B, RAR-Related Orphan Receptor Beta, RZR-Beta, RZRB, Retinoic Acid-Binding Receptor Beta) and RORC (RAR-Related Orphan Receptor C, RAR-Related Orphan Receptor Gamma, RORG, RZR-Gamma, RZRG, Retinoic Acid-Binding Receptor Gamma). We visually inspected the signals for these circadian related genes. The objective was to ascertain if there was a signal that just did not oscillate with a 24 hour frequency or if the signal was either not present or too low to be measured by the probe set. Signal intensities for Bhlhb2, NFIL3A, Clock, RORC, and RORB were sufficiently strong to indicate that they were expressed in the tissue even though they did not have a circadian rhythm. For the remainder of the probe sets, the signal was very low indicating that either they are not expressed in the tissue or that the probe set was not adequate to measure their presence.

Previously we conducted two time series experiments in which cohorts of rats were given MPL either as a single bolus dose or chronic infusion and livers analyzed by gene arrays (Almon et al., 2005; Almon et al., 2007). Because a major regulator of circadian rhythms is the HPA axis, these arrays were examined for clock genes. Figure 5 and 6 show the acute and chronic profiles for both PER2 and BMAL1, two major clock genes. In the acute profile both respond to the single dose with a transient oscillation. With chronic infusion, both genes begin to oscillate but after about 48 hours all points for BMAL1 shows enhanced expression while all points for PER2 shows down-regulation. Three additional clock genes, DBP, nr1d1 and nr1d2, all have acute and chronic profiles similar to PER2 with the chronic profiles being consistently down-regulated after 48 hrs (Figures 7–9).

Although the data suggest that BMAL1 may be continuously up regulated after 48 hours and that PER2, DBP, nr1d1 and nr1d2 may be continuously down regulated after 48 hours, this conclusion may be an artifact of sampling times. If one simply ignores the 36 hour point between 24 hours and 48 hours the conclusion of continuous up or down regulation extends back 24 hours. An alternative possibility is that all continue to oscillate with BMAL1 being out of phase with PER2, DBP, nr1d1 and nr1d2.

Functional groupings

Using extensive literature searches and domain knowledge we parsed all of the genes for which there were probe sets with a 24 hour frequency of oscillation into functional groups. We were able to identify genes that corresponded to all but eleven of the 265 probe sets. In all cases we

attempted to classify the gene with respect to its function in the liver. This categorization is not perfect because some genes can fit into more than one group. For example, we placed interleukin 32 (IL32) and Kruppel-like factor 13 (Klf13) in the Immune Related group, whereas they could also have been placed in the Signaling and Transcription Regulation groups respectively. The thirteen functional groups are as follows: Bile Acid/Cholesterol Biosynthesis; Cell Cycle/Apoptosis; Translation/Protein Processing; Cytoskeleton; Carbohydrate/Glucose Metabolism; Immune Related; Lipid Metabolism; Mitochondrial; Protein Degradation; Signaling; Small Molecule Metabolism; Transcription Regulation; and Other. Table 1 shows the relevant information for each probe set in each functional grouping along with the cluster to which it belongs. As can be seen in Figure 2, Clusters 1 and 2 reach maxima during the light period, Cluster 3 reaches a maximum very close to the transition between light and dark while Clusters 4 and 5 reach maxima during the dark period. The most highly populated functional group is Translation/Protein Processing which contains 65 probe sets. Interestingly 55 of the probe sets are in Clusters 4 and 5 with maxima during the dark period. In contrast, the second most populated functional group is Cell Cycle/Apoptosis with 35 probe sets that are distributed almost equally between Clusters 1 and 2 with maxima during the light period and Clusters 4 and 5 with maxima during the dark period. The next two most populated groups are Lipid Metabolism and Transcription Regulation with 21 probe sets each. Lipid Metabolism has several probe sets in Cluster 3 with most of the remainder in Clusters 4 and 5. This pattern suggests that the system begins to anticipate the active dark period during the end of the light inactive period. Transcription Regulation shows no anticipation but Clusters 4 and 5 clearly dominate. The next two most populated groups are Bile Acid/Cholesterol Biosynthesis and Cytoskeleton, with 16 and 15 probe sets respectively. Quite clearly, Cluster 4 contains major enzymes involved in cholesterol biosynthesis while the production and movement of bile acids seems much more distributed. The remaining functional groups, Signaling (14), Carbohydrate/Glucose metabolism (13), Small Molecule Metabolism (12), Mitochondrial (12), Immune Related (11) and Protein Degradation (6) also have distributions that indicate functional significance during different times of the circadian cycle. The Other category contains 24 probe sets but 11 of these could not be assigned a function.

Drug targets and biomarkers

Three of the functional groups presented in Table 1 were unusually rich in potential drug targets and biomarkers. These functional groups of genes were examined more closely to identify current or potential drug targets and biomarkers, exploring the premise that the use of a drug or measurements of biomarkers may be optimized by taking advantage of circadian variations in the associated gene targets.

Cholesterol/Bile Acid production

Enzymes associated with the synthesis of both cholesterol and bile acids are all in Cluster 4 which has a maximum expression four hours into the animal's dark/active period. This is not particularly surprising since rats, being nocturnal, are active and ingest food during the dark period, thus requiring bile acids during this time. Notable in this cluster are two probe sets for the enzyme HMG-CoA reductase which is the target for statin cholesterol lowering drugs (Stacpoole et al., 1987; Staels, 2006), as well as Sqle, another potential target for hypocholesterolemic drugs (Chugh et al., 2003), and Cyp7a1, which is the rate-limiting enzyme in the conversion of cholesterol to bile acids and is inhibited by fibrates, a class of hypolipidemic drugs (Post et al., 2001). Clusters 1 and 2 (lights on +3 hr and +6 hr, respectively) contain genes that are important to bile acid flow. For example, Cluster 2 contains Abcb11 which mediates the elimination of cytotoxic bile salts from liver cells to bile, and therefore plays a critical role in the generation of bile flow. A variety of drugs inhibit this export pump which can cause drug-induced intrahepatic cholestasis, one of the major causes of hepatotoxicity (Carlton et al., 2004).

Cell Cycle/Apoptosis

Of these 35 genes, almost all are either cancer chemotherapeutic targets or biomarkers relevant to prognosis. They are distributed throughout the light/inactive and dark/active periods and as such are found in all five clusters. Clusters 1 and 2 both peak in the light period. Cluster 1 is particularly rich in both chemotherapeutic targets and biomarkers, including beta tubulin (the main target of paclitaxel) (Tommasi et al., 2007), TXR1 (whose up-regulation impedes taxane-induced apoptosis in tumor cells) (van Amerongen and Berns, 2006), DAPK1 (whose lack of or low levels of expression is associated with highly aggressive metastatic tumors and is also a prognostic marker for disease recurrence) (Fraser and Hupp, 2007), and reprimo (a candidate tumor-suppressor gene whose aberrant methylation is associated with various cancers) (Takahashi et al., 2005). Similar relationships to cancer can be found in the remaining seven genes in Cluster 1. Cluster 2 contains five genes related to apoptosis, including several Bcl-2-binding proteins (Erkan et al., 2005; Zhao et al., 2005). Cluster 3 which peaks close to the light/dark transition contains only one gene, SHMT1, whose polymorphism is related to methotrexate resistance (de Jonge et al., 2005). Clusters 4 and 5 both peak during the dark period. Cluster 4 contains five genes relevant to the control of cell cycle and apoptosis, including Bnip3, whose down-regulation is associated with increased resistance to both 5-fluoro-uracil and gemcitabine (Erkan et al., 2005). Cluster 5 contains six genes. Of particular import is ODC1, the first enzyme in polyamine biosynthesis. Many chemotherapeutic strategies involve inhibition of polyamine biosynthesis and ODC plays a significant role in many of these, which include direct inhibitors of the enzyme often in combination with polyamine uptake inhibitors (Basuroy and Gerner, 2006). In addition, there are therapeutic approaches seeking to silence the ODC gene (Nakazawa et al., 2007). ODC is also a prognostic indicator, with treatment outcome being inversely related to tumor content (Basuroy and Gerner, 2006). This cluster also contains several other genes involved with DNA repair and thus potential targets for cancer therapies.

Translation and Protein Processing

In this last functional group we included all genes directly associated with both translation such as ribosomal proteins and protein processing such as chaperonins which are large molecular assemblies that assist protein folding to the native state. Inhibitors of chaperonins are being assessed as chemotherapeutic agents while enhancers of chaperonin activity are under investigation because misfolded proteins are responsible for a variety of diseases (Fenton and Horwich, 2003; Murphy, 2005; Powers and Workman, 2006; Zheng and Yenari, 2006). Fifty-five of the 65 genes are concentrated in Clusters 4 and 5 which peak in the dark/active period. Cluster 4 includes Hsp70 and three of its partner proteins: Dnaja1; Dnaja2; and Hsj2 (Zheng and Yenari, 2006). It also contains several genes associated with ribosomal synthesis and assembly, one of which, nucleolin, is currently under investigation as a drug target (Sakita-Suto et al., 2007). A nucleolin antisense oligonucleotide is being studied for inhibition of tumor cell proliferation. Cluster 5 is even richer in genes associated with translation and protein processing. Among these are transcripts for 14 proteins with chaperonin activity including Hsp90, the most abundant molecular chaperone in eukaryotic cells and a major focus for drug development (Powers and Workman, 2006). It also contains many genes associated with ribosomes including five transcripts for proteins that are part of the 60S ribosomal subunit. In addition there are transcripts for RNA helicases, several proteins involved in mRNA processing and EIF4A3 (Chan et al., 2004). What is clear from these data is that, for the most part, protein synthesis and processing take place during the dark when the animal is active. However, there are a limited number of transcripts that reach a maximum at other times. For example, the only gene in Cluster 3 is FKBP5 which is both a potential drug target and a biomarker. Its isomerase activity is inhibited by FK506 (tacrolimus), a macrolide immunosuppressant. Allelic variations in the FKBP5 gene are associated with depression and response to antidepressants (Binder et al., 2004). This relationship to depression seems to be related to activity of the HPA axis.

Therefore it is probably relevant that FKBP5 reaches an expression maximum at a time very close to when circulating corticosterone peaks.

DISCUSSION

This report describes an analysis of circadian rhythms of mRNA expression in the liver of adult male rats. Animals were sacrificed at nine times during a 12 hour light period and nine corresponding times during a 12 hour dark period. Liver RNAs from each of the 54 animals were applied to individual Affymetrix GeneChips (RAE230A). Analysis yielded 265 probe sets with a 24 hour frequency. Because of the richness of this dataset, we were able to apply QT clustering and identified 5 groups with maxima at different times during the cycle. Two peaked during the light period, two during the dark period, and one very close to the light to dark transition. Approximately two-thirds of the probe sets reach maximum expression during the active (dark) period. The chip in several cases contained more than one probe set for the same gene. In 14 out of 15 instances, all probe sets for the same gene sorted to the same cluster. The single exception was Pvrl2 which sorted to both Clusters 1 and 2. The correlation coefficient of the probe set in Cluster 1 (1375216_at) was 0.84 while the correlation coefficient of the probe set in Cluster 2 (1370345_at) was also 0.84. Both have amongst the lowest correlations with the centroids of their respective clusters.

Regulation of the central clock involves a number of other transcription factors that may be expressed in peripheral tissues. The array used here contained probe sets for PER1, PER2 and, PER3. However, only PER2 showed significant expression and circadian oscillation while PER1 and PER3 had very low signals. Similarly, probe sets for CRY2 and Bhlhb3 also had very low signals. A very low signal can be due to either the lack of expression of the gene or inadequacy of the probe set to measure the signal. In contrast, the chip contained probe sets for Bhlhb2, NFIL3A, Clock, RORC and RORB, and these signals were reasonably strong but without oscillation. It has been reported that at least in some tissues, Clock is expressed at tonic levels and that cycling is due to the rhymicity of its heterodimeric partner BMAL (Reddy et al., 2005). Of the remaining transcription factors that have been implicated in regulation of circadian changes in gene expression only PER2, BMAL DBP, Nr1d1, and Nr1d2 showed a pattern of circadian oscillation. PER2 was in Cluster 5 during the dark period while BMAL was in Cluster 1 during the light period. DBP, Nr1d1 and Nr1d2 are all in Cluster 3.

The fact that BMAL1, PER2, DBP, Nr1d1 and Nr1d2 all begin to oscillate in response to acute MPL dosing suggest that they are all glucocorticoid sensitive either directly or indirectly. The observation that following chronic dosing an initial oscillation of BMAL occurs followed by what appears to be continuous up-regulation while PER2, DBP, Nr1d1 and Nr1d2 shows oscillation followed by what appears to be continuous down-regulation is potentially informative. However, the apparent continuous up- or down-regulation of the genes may actually be an artifact of sampling times. Just as reasonable an interpretation of the results is that all five genes continue to oscillate throughout the infusion period with BMAL being out of phase with PER2, DBP, Nr1d1 and Nr1d2.

Because synthetic glucocorticoids are a widely used class of drugs, we compared circadian regulated gene expression with those directly regulated by corticosteroids. These datasets together allowed us to address two basic but related questions. The first is: do all genes that respond to corticosteroids have circadian rhythms? The second is: do all genes with circadian rhythms respond to corticosteroid? The answer to both questions is no. Seventy-seven of the genes identified were both circadian and MPL responsive. The fact that all genes that respond to MPL are not circadian and that all genes with circadian rhythms do not respond to MPL suggests that there exist some diversity in mediating mechanisms. This result is consistent with

previously described observations comparing our acute and chronic profiles (Almon et al., 2007).

If an animal is diurnal, changes in mRNA expression near the end of the dark period begins to prepare the animal for the activity and feeding time. Similarly, changes during the end of the light period prepare the diurnal animal for inactivity and rest. Rats are nocturnal and cycling of gene expression in peripheral tissues like the liver is reversed relative to humans who are essentially diurnal. We explored the results with a focus of potential chronotherapeutic insight.

We identified several genes transcripts that are closely associated with hypocholesterolemic drug strategies. Among these are transcripts for HMG-CoA reductase, the statin target, Sqle, involved in cholesterol synthesis, and Cyp7a1 which is the fibrate target in conversion of cholesterol to bile acids. These transcripts are in Cluster 4 which reaches a maximum 4 hr into the animal's dark/active period. The current practice of having patients take statins before they go to bed (Staels, 2006) would seem inappropriate since available data indicates that in humans, HMG-CoA reductase has a maximum expression at about 10 AM (Harwood et al., 1987; Stacpoole et al., 1987). In those experiments the investigators were directly measuring enzymatic activity in serially drawn mononuclear leukocyte. The assumption was that activity in mononuclear leukocyte mirrors activity in the liver. In contrast, whole body cholesterol biosynthesis has been reported to peak between midnight and 3 AM (Parker et al., 1982). In those experiments, the investigators used plasma mevalonic acid as a biomarker for whole body cholesterol biosynthesis. Mevalonic acid is the direct product of HMG-CoA reductase. In addition, urinary mevalonic acid has become an indicator of the effectiveness of statin drug treatment (Hiramatsu et al., 1998). However, our data is consistent with the data of Harwood et al. indicating the enzyme reaches its peak during the animal's active feeding period which in the case of rats would be during the dark period as opposed to the light period in humans. The presence of squalene epoxidase in Cluster 4 further reinforces the validity of these observations. What is confusing is why plasma and urine mevalonic acid peak during the inactive period in humans. Most of the mevalonic acid synthesized in the liver is used for cholesterol and then bile acid biosynthesis. However, the preponderance of mevalonic acid in circulation is metabolized by the kidney with the primary products being squaline and lanosterol (Raskin and Siperstein, 1974). The reason that the timing of the use of statins is important may have less to do with efficacy in lowering cholesterol and more to do with the toxic side effect associated with destabilization of muscle membranes and the development of rhabdomyolysis.

Of the transcripts with circadian rhythms, 35 were for proteins related to cell cycle and apoptosis. In contrast to the cholesterol synthesis related genes, the genes in this functional group are distributed in all five clusters. A relationship between circadian rhythms and cell cycle is well established and our data simply confirms and elaborates on the observations of others. However, the exploitation of these observations in cancer chemotherapy is not straightforward. In cancer therapeutics the important consideration is outcomes, which is based on the balance between toxic and therapeutic effects. If all dividing cells are entrained the same way to the circadian rhythm, then attaining an optimum balance is more complicated. However, some evidence is available that at least in some cases cancer cells have altered organization of the cell cycle relative to the circadian rhythm (Canaple et al., 2003; Garcia-Saenz et al., 2006). To the degree that this is true then knowledge of the circadian expression of drug targets in normal cells may provide a basis for reducing toxicity. Adding to the complexity are the observations that endogenous circadian rhythms are often disrupted in cancer patients.

Of the 265 circadian transcripts, 65 are associated with translation and protein processing. Out of these, only 8 reach a maximum during the light/inactive period. Cluster 3, which reaches a maximum shortly after the transition, contains only one transcript, FKBP5. FKBP5 is

associated with glucocorticoid signaling (Binder et al., 2004) and reaches a maximum expression very close to the maximum of the corticosterone circadian rhythm. Clusters 4 and 5 contain the remaining 55 transcripts. Prominent among these are 20 chaperone related proteins. Both inhibiting and enhancing chaperone activities are evolving drug strategies. An important set of drugs in this category are geldanamycin derivatives which inhibit Hsp90 causing the degradation of proteins involved in a large variety of cellular processes from cell cycle and apoptosis to angiogenesis. Because misfolded proteins are associated with several diseases there are a variety of approaches being developed to enhance the activity of Hsp90 and other chaperonins (Powers and Workman, 2006). Two particularly interesting areas are chaperone-mediated enzyme enhancement and gene therapy. What is also clear is that protein synthesis related expression occurs primarily in Cluster 5. The fact that six proteins that are part of the 60S ribosomal subunit are co-expressed in Cluster 5 tends to validate our results. Proteins that work together are expressed together.

With the burgeoning development of antisense oligonucleotides it is probable that more transcripts will become drug targets. Timing will be an important aspect in the use of antisense technology when applied to transcripts with circadian rhythms.

Supplementary Material

Refer to Web version on PubMed Central for supplementary material.

Acknowledgements

This dataset was developed at the Children's National Medical Center under the auspices of a grant from the National Heart, Lung, and Blood Institute (NHLBI)/NIH Programs in Genomic Applications HL 66614 (Eric P. Hoffman, PI). We would like to acknowledge the technical assistance of Ms. Nancy Pyszczynski and Ms. Suzette Mis.

This work was supported by grant GM 24211 from the National Institute of General Medical Sciences, NIH, Bethesda, MD. EY and IPA also acknowledge support from NSF grant 0519563 and EPA grant GAD R 832721-010.

Abbreviations

ADX
: adrenalectomized

MPL
: methylprednisolone

SCN
: suprachiasmic nucleus

References

Almon RR, Dubois DC, Jin JY, Jusko WJ. Pharmacogenomic responses of rat liver to methylprednisolone: an approach to mining a rich microarray time series. AAPS Journal 2005;7:E156–194. [PubMed: 16146338]

Almon RR, DuBois DC, Jusko WJ. A microarray analysis of the temporal response of liver to methylprednisolone: a comparative analysis of two dosing regimens. Endocrinology 2007;148:2209–2225. [PubMed: 17303664]

Badiu C. Genetic clock of biologic rhythms. Journal of Cellular & Molecular Medicine 2003;7:408–416. [PubMed: 14754509]

Basuroy UK, Gerner EW. Emerging concepts in targeting the polyamine metabolic pathway in epithelial cancer chemoprevention and chemotherapy. Journal of Biochemistry 2006;139:27–33. [PubMed: 16428316]

Binder EB, Salyakina D, Lichtner P, Wochnik GM, Ising M, Putz B, Papiol S, Seaman S, Lucae S, Kohli MA, Nickel T, Kunzel HE, Fuchs B, Majer M, Pfennig A, Kern N, Brunner J, Modell S, Baghai T, Deiml T, Zill P, Bondy B, Rupprecht R, Messer T, Kohnlein O, Dabitz H, Bruckl T, Muller N, Pfister H, Lieb R, Mueller JC, Lohmussaar E, Strom TM, Bettecken T, Meitinger T, Uhr M, Rein T, Holsboer F, Muller-Myhsok B. Polymorphisms in FKBP5 are associated with increased recurrence of depressive episodes and rapid response to antidepressant treatment. Nature Genetics 2004;36:1319–1325. [PubMed: 15565110]

Canaple L, Kakizawa T, Laudet V. The days and nights of cancer cells. Cancer Research 2003;63:7545–7552. [PubMed: 14633665]

Carlton VEH, Pawlikowska L, Bull LN. Molecular basis of intrahepatic cholestasis. Annals of Medicine 2004;36:606–617. [PubMed: 15768832]

Challet E, Caldelas I, Graff C, Pevet P. Synchronization of the molecular clockwork by light- and food-related cues in mammals. Biological Chemistry 2003;384:711–719. [PubMed: 12817467]

Chan CC, Dostie J, Diem MD, Feng W, Mann M, Rappsilber J, Dreyfuss G. eIF4A3 is a novel component of the exon junction complex. Rna-A Publication of the Rna Society 2004;10:200–209.

Chugh A, Ray A, Gupta JB. Squalene epoxidase as hypocholesterolemic drug target revisited. Progress in Lipid Research 2003;42:37–50. [PubMed: 12467639]

Dardente H, Klosen P, Caldelas I, Pevet P, Masson-Pevet M. Phenotype of Per1- and Per2-expressing neurons in the suprachiasmatic nucleus of a diurnal rodent (Arvicanthis ansorgei): comparison with a nocturnal species, the rat. Cell & Tissue Research 2002;310:85–92. [PubMed: 12242487]

de Jonge R, Hooijberg JH, van Zelst BD, Jansen G, van Zantwijk CH, Kaspers GJL, Peters GJ, Ravindranath Y, Pieters R, Lindemans J. Effect of polymorphisms in folate-related genes on in vitro methotrexate sensitivity in pediatric acute lymphoblastic leukemia. Blood 2005;106:717–720. [PubMed: 15797993]

Erkan M, Kleeff J, Esposito I, Giese T, Ketterer K, Buchler MW, Giese NA, Friess H. Loss of BNIP3 expression is a late event in pancreatic cancer contributing to chemoresistance and worsened prognosis. Oncogene 2005;24:4421–4432. [PubMed: 15856026]

Fenton WA, Horwich AL. Chaperonin-mediated protein folding: fate of substrate polypeptide. Quarterly Reviews of Biophysics 2003;36:229–256. [PubMed: 14686103]

Fraser JA, Hupp TR. Chemical genetics approach to identify peptide ligands that selectively stimulate DAPK-1 kinase activity. Biochemistry 2007;46:2655–2673. [PubMed: 17297916]

Garcia-Saenz JA, Martin M, Maestro M, Vidaurreta M, Veganzones S, Villalobos L, Rodriguez-Lajusticia L, Rafael S, Sanz-Casla MT, Casado A, Sastre J, Arroyo M, Diaz-Rubio E. Circulating tumoral cells lack circadian-rhythm in hospitalized metastasic breast cancer patients. Clinical & Translational Oncology: Official Publication of the Federation of Spanish Oncology Societes & of the National Cancer Institute of Mexico 2006;8:826–829.

Harwood HJ Jr, Bridge DM, Stacpoole PW. In vivo regulation of human mononuclear leukocyte 3-hydroxy-3-methylglutaryl coenzyme A reductase. Studies in normal subjects. Journal of Clinical Investigation 1987;79:1125–1132. [PubMed: 3558818]

Haughey DB, Jusko WJ. Analysis of methylprednisolone, methylprednisone and corticosterone for assessment of methylprednisolone disposition in the rat. Journal of Chromatography A 1988;430:241–248.

Hiramatsu M, Hayashi A, Hidaka H, Ueshima H, Kanno T. Enzyme immunoassay of urinary mevalonic acid and its clinical application. Clin Chem 1998;44:2152–2157. [PubMed: 9761249]

Labrecque G, Bureau JP, Reinberg AE. Biological rhythms in the inflammatory response and in the effects of non-steroidal anti-inflammatory drugs. Pharmacology & Therapeutics 1995;66:285–300. [PubMed: 7667399]

Murphy PJM. Regulation of glucocorticoid receptor steroid binding and trafficking by the hsp90/hsp70-based chaperone machinery: implications for clinical intervention. Leukemia 2005;19:710–712. [PubMed: 15759036]

Nakazawa K, Nemoto T, Hata T, Seyama Y, Nagahara S, Sano A, Itoh H, Nagai Y, Kubota S. Single-injection ornithine decarboxylase-directed antisense therapy using atelocollagen to suppress human cancer growth. Cancer 2007;109:993–1002. [PubMed: 17318877]

Oishi K, Miyazaki K, Kadota K, Kikuno R, Nagase T, Atsumi G-i, Ohkura N, Azama T, Mesaki M, Yukimasa S, Kobayashi H, Iitaka C, Umehara T, Horikoshi M, Kudo T, Shimizu Y, Yano M, Monden M, Machida K, Matsuda J, Horie S, Todo T, Ishida N. Genome-wide expression analysis of mouse liver reveals CLOCK-regulated circadian output genes. Journal of Biological Chemistry 2003;278:41519–41527. [PubMed: 12865428]

Parker TS, McNamara DJ, Brown C, Garrigan O, Kolb R, Batwin H, Ahrens EH. Mevalonic acid in human plasma: relationship of concentration and circadian rhythm to cholesterol synthesis rates in man. Proc Natl Acad Sci 1982;79:3037–3041. [PubMed: 6953446]

Post SM, Duez H, Gervois PP, Staels B, Kuipers F, Princen HM. Fibrates suppress bile acid synthesis via peroxisome proliferator-activated receptor-alpha-mediated downregulation of cholesterol 7alpha-hydroxylase and sterol 27-hydroxylase expression. Arteriosclerosis, Thrombosis & Vascular Biology 2001;21:1840–1845.

Powers MV, Workman P. Targeting of multiple signalling pathways by heat shock protein 90 molecular chaperone inhibitors. Endocrine-Related Cancer 2006;13(Suppl 1):S125–135. [PubMed: 17259553]

Raskin P, Siperstein MD. Mevalonate metabolism by renal tissue in vivo. J Lipid Research 1974;15:20–25. [PubMed: 4811213]

Reddy AB, Wong GKY, O'Neill J, Maywood ES, Hastings MH. Circadian clocks: neural and peripheral pacemakers that impact upon the cell division cycle. Mutation Research 2005;574:76–91. [PubMed: 15914209]

Reinberg AE. Concepts in chronopharmacology. Annual Review of Pharmacology & Toxicology 1992;32:51–66.

Sakita-Suto S, Kanda A, Suzuki F, Sato S, Takata T, Tatsuka M. Aurora-B regulates RNA methyltransferase NSUN2. Molecular Biology of the Cell 2007;18:1107–1117. [PubMed: 17215513]

Smolensky MH, Reinberg AE, Martin RJ, Haus E. Clinical chronobiology and chronotherapeutics with applications to asthma. Chronobiology International 1999;16:539–563. [PubMed: 10513882]

Stacpoole PW, Bridge DM, Alvarez IM, Goldberg RB, Harwood HJ Jr. In vivo regulation of human mononuclear leukocyte 3-hydroxy-3-methylglutaryl coenzyme A reductase. Decreased enzyme catalytic efficiency in familial hypercholesterolemia. Journal of Clinical Investigation 1987;80:1401–1408. [PubMed: 2824560]

Staels B. When the Clock stops ticking, metabolic syndrome explodes. Nature Medicine 2006;12:54–55.discussion 55

Takahashi T, Suzuki M, Shigematsu H, Shivapurkar N, Echebiri C, Nomura M, Stastny V, Augustus M, Wu C-W, Wistuba II, Meltzer SJ, Gazdar AF. Aberrant methylation of Reprimo in human malignancies. International Journal of Cancer 2005;115:503–510.

Tommasi S, Mangia A, Lacalamita R, Bellizzi A, Fedele V, Chiriatti A, Thomssen C, Kendzierski N, Latorre A, Lorusso V, Schittulli F, Zito F, Kavallaris M, Paradiso A. Cytoskeleton and paclitaxel sensitivity in breast cancer: the role of beta-tubulins. International Journal of Cancer 2007;120:2078–2085.

Ueda HR, Hayashi S, Chen W, Sano M, Machida M, Shigeyoshi Y, Iino M, Hashimoto S. System-level identification of transcriptional circuits underlying mammalian circadian clocks. Nature Genetics 2005;37:187–192. [PubMed: 15665827]

van Amerongen R, Berns A. TXR1-mediated thrombospondin repression: a novel mechanism of resistance to taxanes? Genes & Development 2006;20:1975–1981. [PubMed: 16882973]

Zhao X, Ayer RE, Davis SL, Ames SJ, Florence B, Torchinsky C, Liou JS, Shen L, Spanjaard RA. Apoptosis factor EI24/PIG8 is a novel endoplasmic reticulum-localized Bcl-2-binding protein which is associated with suppression of breast cancer invasiveness. Cancer Research 2005;65:2125–2129. [PubMed: 15781622]

Zheng Z, Yenari MA. The application of HSP70 as a target for gene therapy. Frontiers in Bioscience 2006;11:699–707. [PubMed: 16146762]

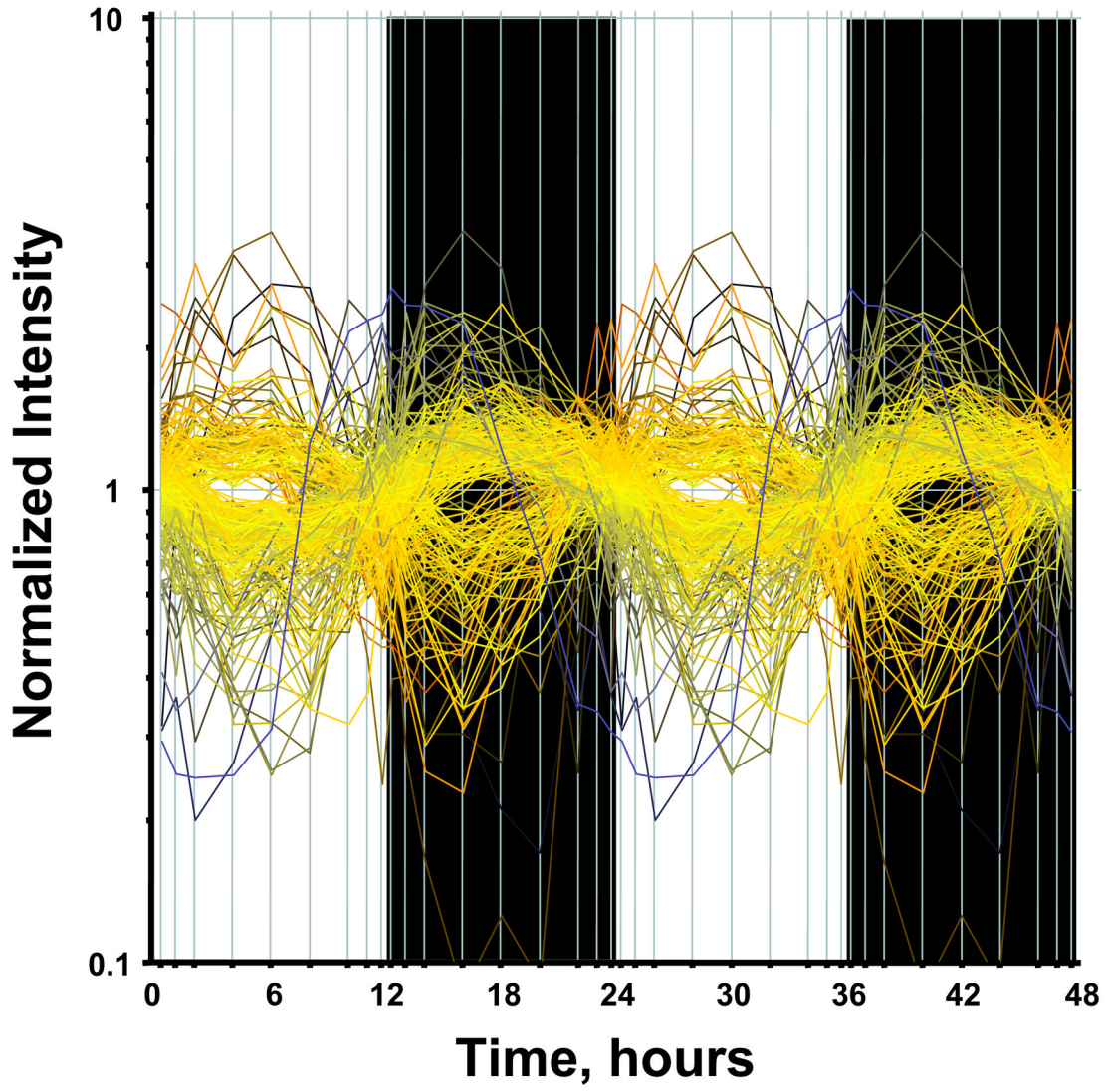

Figure 1.
Expression of circadian regulated genes. A non-linear curve fit using MATLAB was conducted which fitted a sinus function [A*sin(Bt + c)] to the data including the replicates. Genes that could be curve fitted with a R2 correlation of greater than 0.8 were kept.

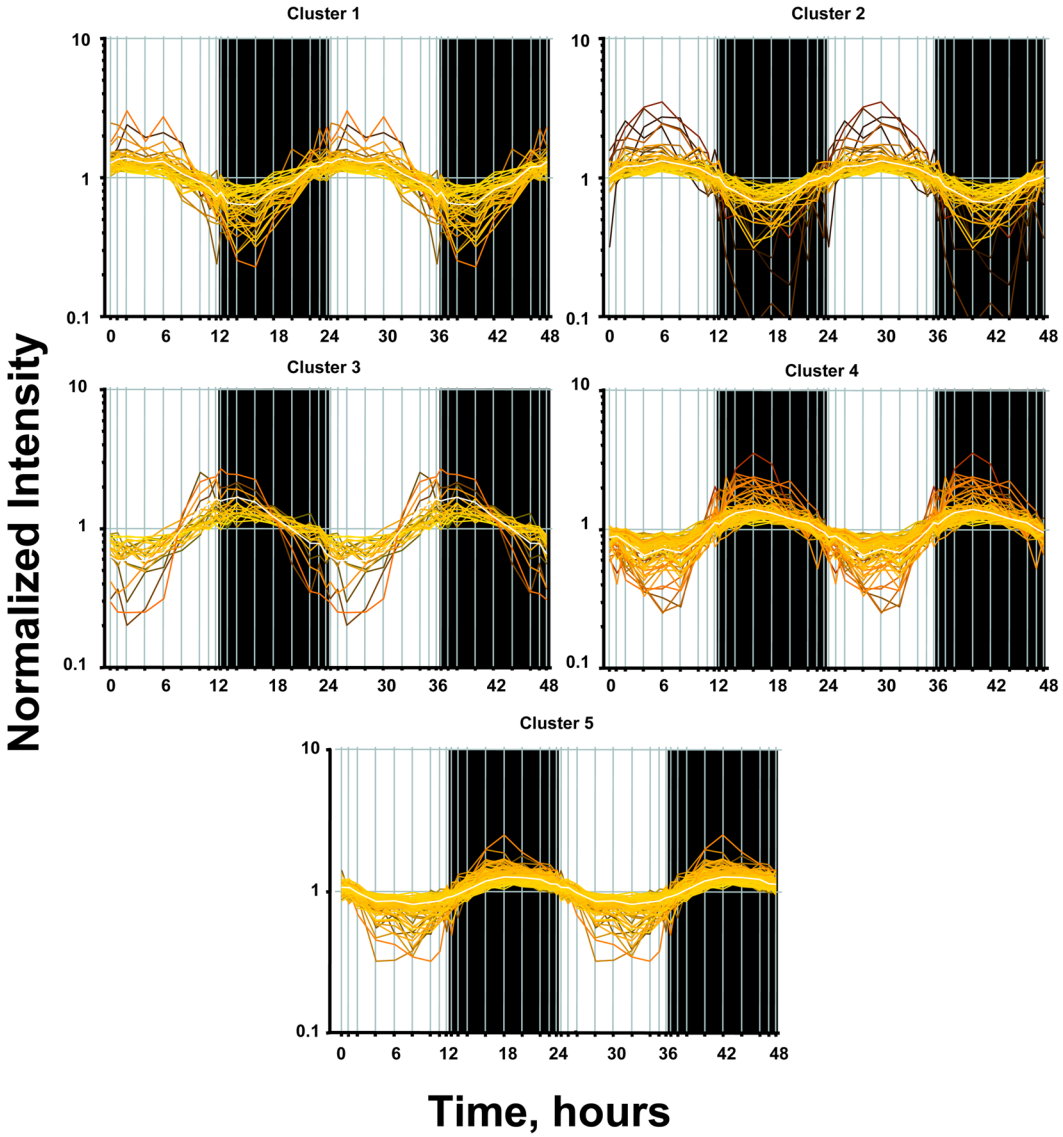

Figure 2.
QT clustering of circadian regulated genes. Each probe set has greater than a .75 Person's correlation with the centroid of the cluster (shown in white0.

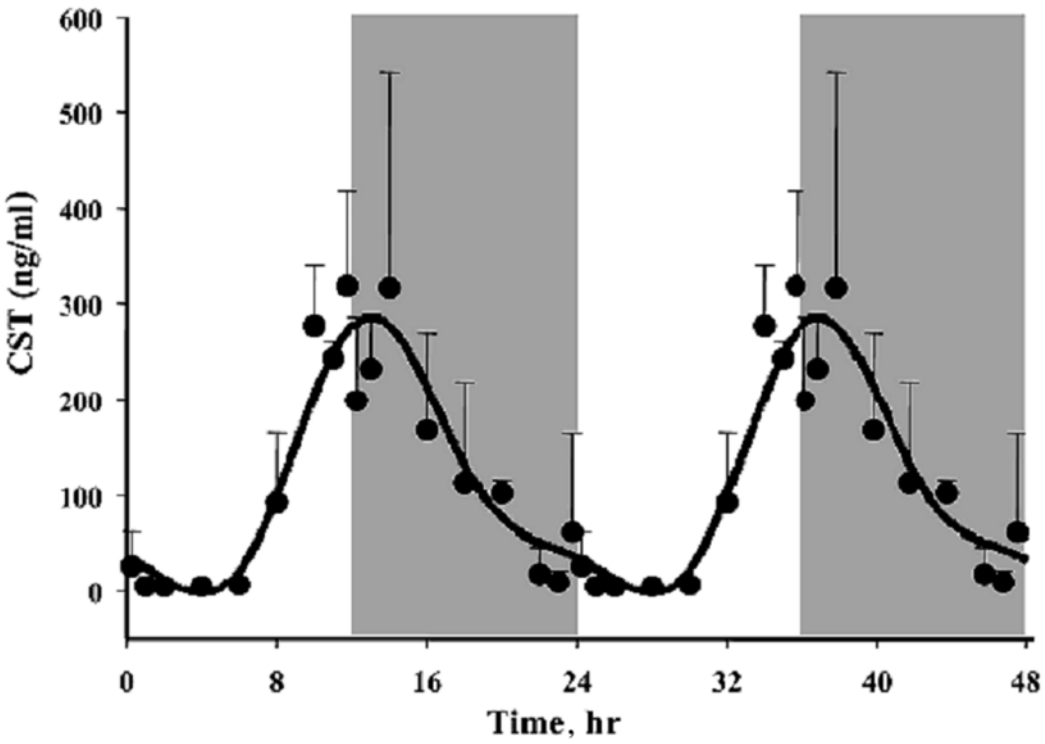

Figure 3.
Plasma corticosterone (CST) as a function of circadian time as measured by HPLC. Symbols represent means and error bars 1 sd of the mean. Unshaded areas indicate light period and shaded areas indicate dark period.

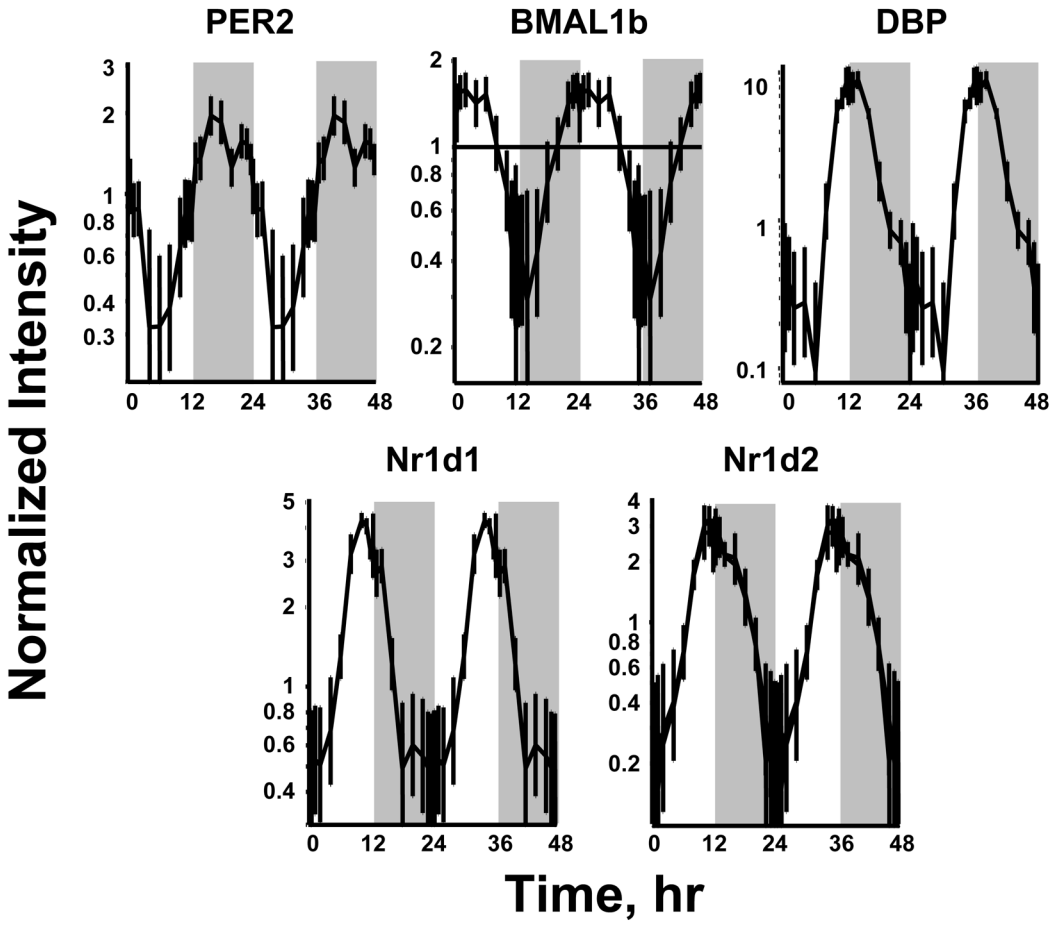

Figure 4.
Expression patterns of 5 clock related transcription factors in liver as a function of circadian time. Unshaded areas indicate light periods and shaded areas indicate dark periods.

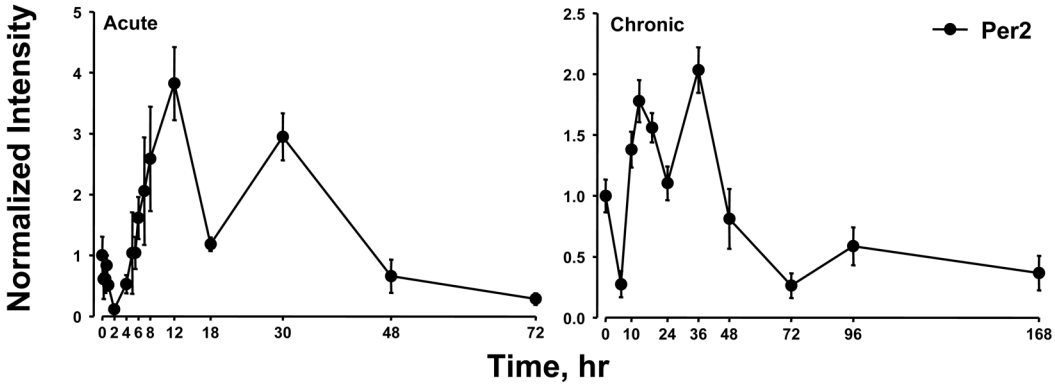

Figure 5.

Expression patterns of PER2 as a function of time after MPL administration to adrenalectomized animals. Left panels present data from acute (bolus 50 mg/kg) MPL dosing; right panels present data from chronic (0.3 mg/kg/h) MPL infusion. Array signals are normalized to zero time control values, and plotted as mean relative intensity at each time point. Error bars represent 1 sd of the mean.

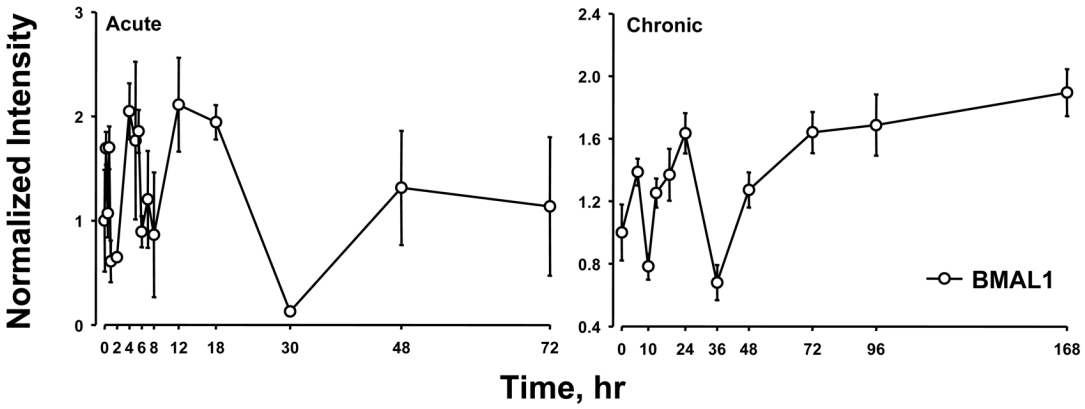

Figure 6.

Expression patterns of BMAL1 as a function of time after MPL administration to adrenalectomized animals. Left panels present data from acute (bolus 50 mg/kg) MPL dosing; right panels present data from chronic (0.3 mg/kg/h) MPL infusion. Array signals are normalized to zero time control values, and plotted as mean relative intensity at each time point. Error bars represent 1 sd of the mean.

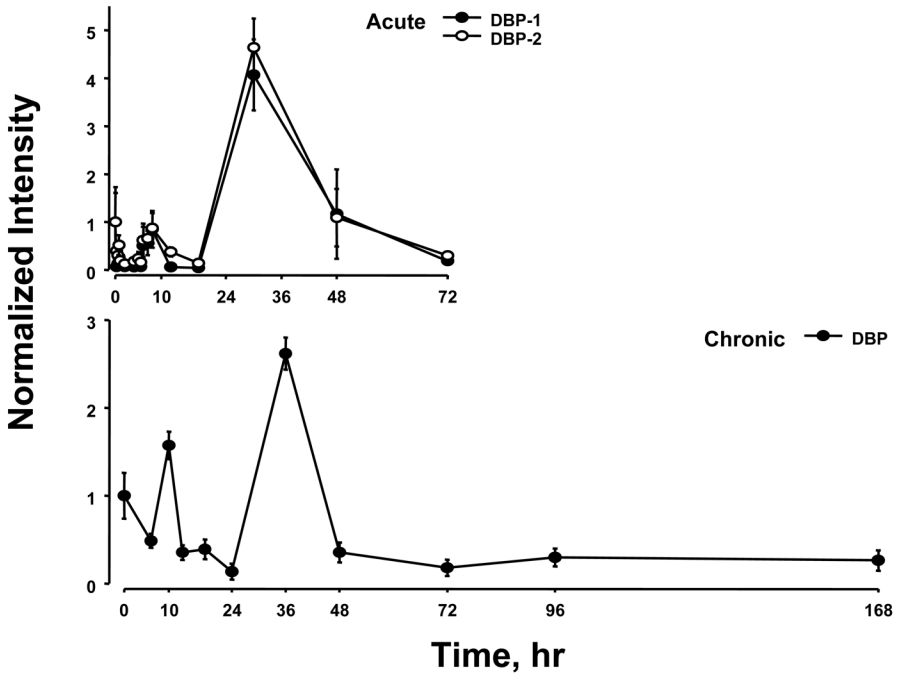

Figure 7.

Expression patterns of DBP as a function of time after MPL administration to adrenalectomized animals. Upper panel presents data from acute (bolus 50 mg/kg) MPL dosing; lower panel presents data from chronic (0.3 mg/kg/h) MPL infusion. Array signals are normalized to zero time control values, and plotted as mean relative intensity at each time point. Error bars represent 1 sd of the mean. The array used for the acute experiments contained 2 probe sets for DBP, and both are presented.

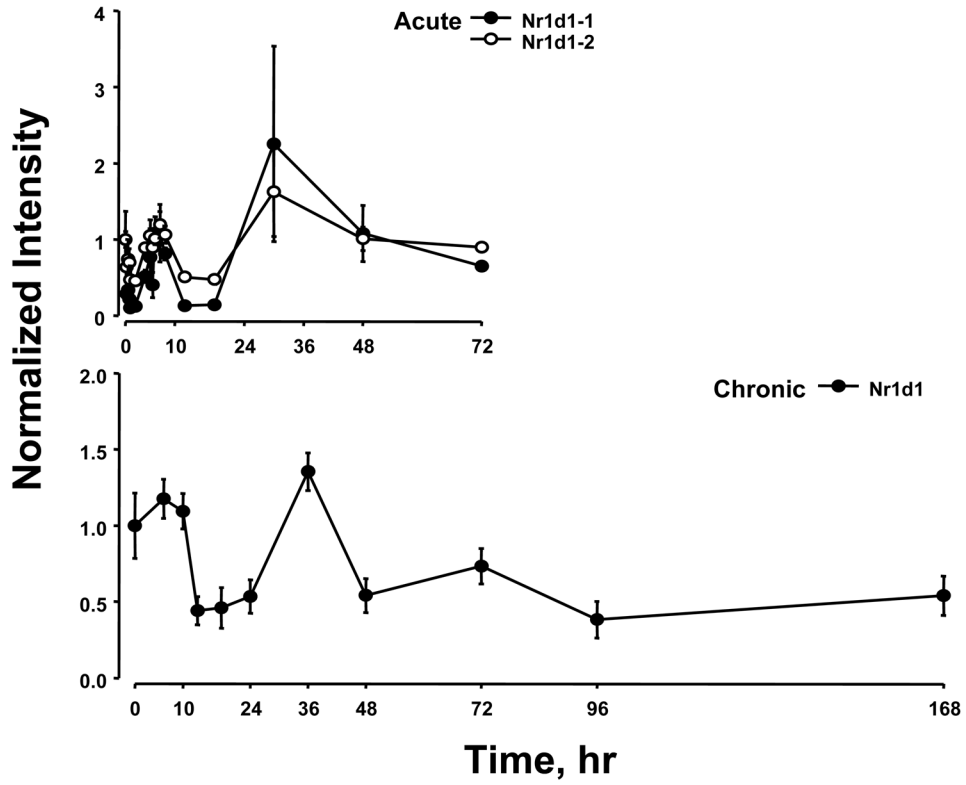

Figure 8.

Expression patterns of Nr1d1 as a function of time after MPL administration to adrenalectomized animals. Upper panel presents data from acute (bolus 50 mg/kg) MPL dosing; lower panel presents data from chronic (0.3 mg/kg/h) MPL infusion. Array signals are normalized to zero time control values, and plotted as mean relative intensity at each time point. Error bars represent 1 sd of the mean. The array used for the acute experiments contained 2 probe sets for Nr1d1, and both are presented.

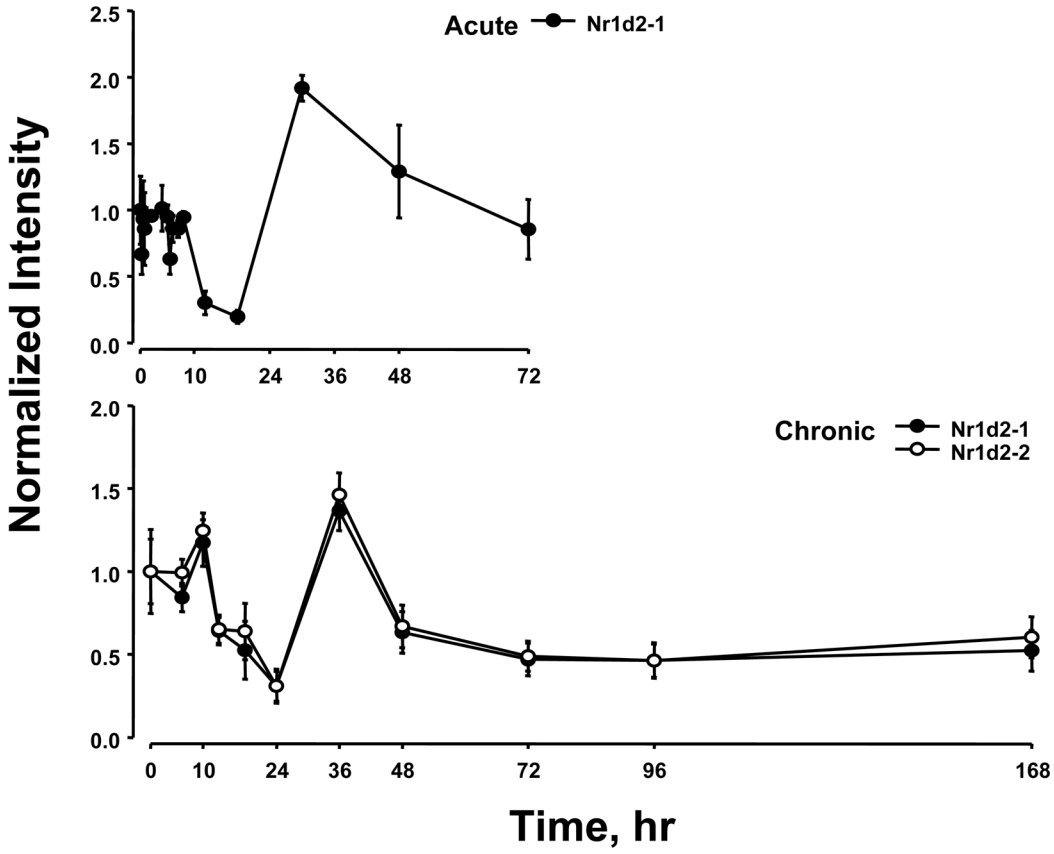

Figure 9.

Expression patterns of Nr1d2 as a function of time after MPL administration to adrenalectomized animals. Upper panel presents data from acute (bolus 50 mg/kg) MPL dosing; lower panel presents data from chronic (0.3 mg/kg/h) MPL infusion. Array signals are normalized to zero time control values, and plotted as mean relative intensity at each time point. Error bars represent 1 sd of the mean. The array used for the chronic experiments contained 2 probe sets for Nr1d2, and both are presented.

Table 1

Functional Characterization of Circadian Regulated Genes in Liver.

Probe ID	Accession No.	Cluster	Symbol	Gene Name	Gene Function
Translation/Protein Processing					
1377192_a_at	BM384629	1	Clpx	caseinolytic peptidase X	protein chaperone to mitochondria
1372536_at	AI105042	1	Cabc1	chaperone, ABC1 activity of bc1 complex like	p53 induced chaperone, for protein complexes in the respiratory chain
1390107_at	BG670294	1	Sytl2	synaptotagmin-like 2	vesicle trafficking
1386918_a_at	AF087827	1	Oprs1	opioid receptor, sigma 1	export of lipids fromER to plasma membrane
1389965_at	AA799818	2	Tgoln2	trans-Golgi network protein 2	key sorting station for proteins, membrane traffic in secretory pathway
1390697_at	BI278125	2	Gemin8	gem (nuclear organelle) associated protein 8	small nuclear ribonucleoprotein assembly
1373730_at	BI282077	2	RBM33	RNA binding motif protein 33	RNA binding
1367537_at	AI012479	2	Eif4enif1	eukaryotic translation initiation factor 4E nuclear import factor 1	translation
1398994_at	BI301193	2	Tpst2	protein-tyrosine sulfotransferase 2	posttranslational modification
1388901_at	AW534837	3	Fkbp5	FK506 binding protein 5	glucocorticoid signaling, HSP90
1398240_at	NM_024351	4	Hsp70	heat shock protein 70; heat shock 70kD protein 8	molecular chaperone, assists in the correct folding of other proteins
1398819_at	NM_022934	4	Hsj2, Dnaja1, Hsp40	DNAJ (Hsp40) homolog, subfamily A, member 1	partners for Hsp70 chaperones
1387780_at	NM_032079	4	Dnaja2	DNAJ (Hsp40) homolog, subfamily A, member 2	partners for Hsp70 chaperones
1368852_at	BG668811	4	Hsj2	DNAJ-like 2 heat-shock 40-KD protein 4	partners for Hsp70 chaperones
1372141_at	BI289500	4	PFDN2	prefoldin subunit 2	molecular chaperone, assists in the correct folding of other proteins
1388136_at	BF282660	4	Timm9	translocase of inner mitochondrial membrane 9	import and insertion of hydrophobic proteins into mitochondrial inner membrane
1372533_at	AI175790	4	EDEM1	ER degradation enhancer, mannosidase alpha-like 1	accelerates degradation of misfolded proteins in ER
1372085_at	AI237657	4	Arl6ip2	DP-ribosylation factor-like 6 interacting protein 2	translocation of proteins across the ER membrane
1371843_at	AI234128	4	Yipf5	Yip1 domain family, member 5	intracellular trafficking Golgi, Rab GTPases
1374903_at	AI234819	4	Ignt3	beta-1,6-acetylglucosaminyltransferase family polypeptide 3	Golgi, glycoprotein synthesis
1371580_at	AI102725	4	Spfh1	SPFH domain family, member 1	ER lipid raft associated 1
1372642_at	BE113397	4	RNU17A	E1 small nucleolar RNA gene	interact directly with unique segments of pre-rRNA
1374288_at	BG374267	4	FTSJ3	FtsJ homolog 3 (E. coli)	nucleolar, ribosome assembly, rRNA methyltransferase 3
1398832_at	NM_012749	4	Ncl	nucleolin	transcription of ribosomal RNA genes by RNA polymerase I, in ribosome maturation
1371498_at	AI412685	4	JTV1, p38	tRNA synthetase cofactor p38	transcription of genes encoding mRNA
1373668_at	BG373075	4	Polr2i	polymerase (RNA) II polypeptide I	DNA directed
1371463_at	AI233239	4	phf5a	PHD finger protein 5A	pre-mRNA splicing, transcriptional regulator
1371596_at	AI008971	4	Rnps1	ribonucleic acid binding protein S1	regulates alternative splicing of a variety of pre-mRNAs
1389301_at	AI176665	4	MBNL1	muscle blind-like 2 isoform 1	triplet-expansion RNA-binding protein
1371372_at	AA944161	5	p23	prostaglandin E synthase 3, telomerase-binding protein p23, Hsp90 co-chaperone	heat-shock protein-90 chaperone p23, coupled to prostaglandin-endoperoxide H synthase-1
1398877_at	BI283691	5	Stip1	stress-induced phosphoprotein 1	association of the molecular chaperones HSP70 and HSP90
1368049_at	NM_012670	5	Tcp1	T-complex 1	cytosolic chaperone, role in folding of newly translated proteins in cytosol

Probe ID	Accession No.	Cluster	Symbol	Gene Name	Gene Function
1371403_at	AA799545	5	Cct3	chaperonin subunit 3 (gamma)	chaperone, VHL protein (tumor suppressor)
1383160_at	AA892238	5	Chordc1	cysteine and histidine-rich domain(CHORD)-containing, zinc-bp1	binds to HSP90
1388898_at	AI236601	5	Hsph1	heat shock 105kDa/110kDa protein 1	chaperone activity
1375335_at	BI285700	5	Hsp90	heat shock 90kDa protein 1, beta	chaperone activity
1375336_at	AI237389	5	hsp84	heat shock protein 84	chaperone activity
1372701_at	AI237597	5	Hsp1a	heat shock protein 1, alpha	chaperone activity
1372489_at	AI172498	5	Slap	sarcolemma associated protein	chaperone activity
1388331_at	BG057543	5	Hsp90B1	heat shock protein 90kDa beta (Grp94), member 1(HSP90B1)	chaperone activity
1371435_at	BI279561	5	Naca	nascent-polypeptide-associated complex alpha polypeptide	chaperone/stress, prevents inappropriate targeting of non-secretory polypeptides
1371693_at	AA849757	5	AHSA1	activator of heat shock 90kDa protein ATPase homolog 1	stimulated the intrinsic ATPase activity of HSP90
1367686_at	NM_030835	5	RAMP4, SERP1	ribosome associated membrane protein 4	stabilization of membrane proteins in response to stress
1373319_at	BF419628	5	Ddx1	DEAD (Asp-Glu-Ala-Asp) box polypeptide 1	RNA helicases, influence initiation, splicing, and ribosome and splicesome assembly
1367480_at	AI230248	5	Dhx15, EIF4A3	DEAD (Asp-Glu-Ala-Asp) box polypeptide 48	eukaryotic translation initiation factor 4A, isoform 3
1398937_at	BI279381	5	Dhx15	DEAH (Asp-Glu-Ala-His) box polypeptide 15	ATP-dependent RNA helicase, pre-mRNA splicing factor
1388528_at	AW433875	5	Fbl	fibrillarin	component of nucleolar small nuclear ribonucleoprotein particle, processing preribosomal RNA
1371505_at	BG381750	5	Hnrpc	heterogeneous nuclear ribonucleoprotein C	mRNA (pre-mRNA) major constituents of ribonucleoprotein particles
1371957_at	BM388851	5	IMP4	IMP4, U3 small nucleolar ribonucleoprotein	ribosomal protein
1371445_at	BF285649	5	p34	leucine-rich-repeat-protein superfamily; p34 protein, ribosome binding	ribosome binding
1375181_at	AI170643	5	Rpl12	ribosomal protein L12	60S ribosomal subunit
1398315_at	AA800007	5	Rpl15	ribosomal protein L15	60S ribosomal subunit
1398871_at	BG671311	5	Rpl17	ribosomal protein L17	60S ribosomal subunit
1398885_at	AA925327	5	Rpl23	ribosomal protein L23	60S ribosomal subunit
1398749_at	NM_022510	5	Rpl4	ribosomal protein L4	60S ribosomal subunit
1398761_at	NM_031099	5	Rpl5	ribosomal protein L5	chaperone for 5S rRNA
1367606_at	NM_017153	5	Rpls3a	ribosomal protein S3a	ribosome biogenesis; protein biosynthesis
1388117_at	AI411893	5	Snrpb	small nuclear ribonucleoprotein polypeptides B and B1 (Snrpb)	pre-mRNA splicing
1376252_at	AI145784	5	SRp20, Sfrs3	splicing factor, arginine/serine-rich 3 (SRp20) (Sfrs3)	SR family of mRNA splicing factors, consecutive serine (S) and arginine (R) dipeptides
1389344_at	BE109258	5	Usp39	ubiquitin specific protease 39	possible competitor of ubiquitin C-terminal hydrolases (UCHs)
1388424_at	AI407015	5	Eif3s1	eukaryotic translation initiation factor 3, subunit 1 alpha	Translation
1373913_at	BF282271	5	Pnpt1	polyribonucleotide nucleotidyltransferase 1	exosome complex, 3′ to 5′ exoribonuclease activity, RNA processing & degradation
1372688_at	BI296190	5	Exosc7	exosome component 7	rapid degradation of ARE-containing RNAs
1398896_at	AA892567	5	Arcn1	archain 1	coatomer associates with Golgi, biosynthetic protein transport from the ER
1370305_at	U96490	5	Yif1p	Yip1 interacting factor homolog A(YIF1A)	interacts with Yip1
Cell Cycle/Apoptosis					
1367867_at	NM_013222	1	Gfer, ALR	augmenter of liver regeneration; growth factor, erv1-like	induced expression of ODC and AMD1 (polyamine biosynthesis)

Probe ID	Accession No.	Cluster	Symbol	Gene Name	Gene Function
1376788_at	AA818353	1	Dapk1	death associated protein kinase 1	apoptosis positive mediators induced by gamma-interferon
1388484_at	BI296084	1	UBE2C	ubiquitin-conjugating enzyme E2C	regulated destruction of mitotic cyclins A and B
1389408_at	BG379338	1	Rrm2	ribonucleotide reductase M2	formation of deoxyribonucleotides from corresponding ribonucleotides
1390117_at	BG372455	1	Ypel2	yippee-like 2 (Drosophila)	cell division
1390381_at	BG379358	1	Xpc	xeroderma pigmentosum, complementation group C	DNA repair
1390672_at	BG381258	1	RPRM	Reprimo	involved inp53-induced G2 cell cycle arrest
1373542_at	BM386306	1	Sphk2	sphingosine kinase 2 (Sphk2)	formation of sphingosine 1-phosphate (SPP)
1374747_at	BM384279	1	PFTK1	PFTAIRE protein kinase 1	cyclin-dependent kinase related
1388408_at	AA800199	1	Prr13	proline rich 13	regulator of thrombospondin-1, taxol sensativity
1368227_at	NM_031664	1	Slc28a2	solute carrier family 28 (sodium-coupled nucleoside transporter) a2	purine nucleoside transport
1369902_at	NM_139258	2	Bmf	Bcl-2 modifying factor	proapoptotic members of the BCL2 family
1370345_at	L11995	2	Ccnb1	cyclin B	complexes with p34(cdc2) to form the mitosis-promoting factor
1370374_at	AF335281	2	STEAP3	STEAP family member 3	downstream of p53 to interface apoptosis and cell cycle progression
1388642_at	AI412114	2	EI24	etoposide induced 2.4	apoptosis, p53-induced genes
1373722_at	BE111697	2	Kif20a	kinesin family member 20A_	motor-driven transport processes that occur in mitotic cells
1371632_at	AI231166	2	CORO1C	Coronin, actin binding protein 1C	WD repeats
1374939_at	BE112927	2	Cyfip2	cytoplasmic FMR1 interacting protein 2	CYFIP2 is a direct p53 target responsible for p53-dependent apoptosis
1368294_at	NM_053907	2	Dnase1l3	DNase gamma; deoxyribonuclease I-like 3	apoptosis
1374820_at	AI598946	4	L3MBTL4	l(3)mbt-like 4 (Drosophila)	changes in chromatin organization, cell cycle
1375280_at	AW913871	4	PNAS-4	apoptosis-related protein PNAS-4	protein targeting
1387805_at	NM_053420	4	Bnip3	BCL2/adenovirus E1B 19 kDa-interacting protein 3	pro-apoptotic mitochondrial protein
1389738_at	AA848420	4	Ung	uracil-DNA glycosylase	DNA repair enzyme
1387244_at	NM_053899	4	Cgr19	cell growth regulatory with ring finger domain	p53 related, inhibits growth
1367983_at	NM_053430	5	Fen1	flap structure-specific endonuclease 1	removes 5-prime overhanging flaps in DNA repair and synthesis
1370163_at	BF281299	5	Odc1	ornithine decarboxylase 1	cell cycle, biosynthesis of polyamines
1371418_at	BG665035	5	CCT2	chaperonin containing TCP1, subunit 2 (beta)	cyclin E accumulation, partner of cyclin-dependent kinase 2, positive control G1/S transition
1387062_a_at	NM_080400	5	Chek1	checkpoint kinase 1	timing of cell cycle transitions, DNA damage checkpoint
1389384_at	BE111733	5	Hrpap20	hormone-regulated proliferation associated protein 20	phosphoprotein required for proliferation and survival of hormone-dependent tumor cells
1389658_at	BI283104	5	Nsun2	NOL1/NOP2/Sun domain family, member 2	methyltransferase, disassembly nucleolus during mitosis, methylates RNA polymerase III
1388629_at	BF281278	5	Impdh2	inosine 5-monophosphate dehydrogenase 2	de novo synthesis of guanine nucleotides, regulation of cell growth
1369962_at	NM_031014	5	Atic	5-aminoimidazole-4-carboxamide ribonucleotide formyltransferase/IMP cyclohydrolase	de novo purine biosynthesis
1373625_at	AI412012	3	Shmt1	serine hydroxymethyl transferase 1 (soluble)	folate metabolism; biosynthesis of nucleotides and amino acids
1373718_at	BM384071	1	TUBB2	tubulin, beta 2	microtubules cytoskeleton

Probe ID	Accession No.	Cluster	Symbol	Gene Name	Gene Function
1398317_at	BF283428	5	Bpnt1	bisphosphate 3′-nucleotidase 1	nucleotide metabolism
Lipid Metabolism					
1374570_at	AI012474	1	Agpat2	1-acylglycerol-3-phosphate O-acyltransferase 2	signal transduction and lipid biosynthesis
1389377_at	AA851803	1	Insig2	insulin induced gene 2	blocks proteolytic activation of SREBPs by SCAP
1367718_at	NM_017177	2	Chetk	choline kinase-like; choline/ethanolamine kinase	first enzyme in phosphatidylcholine biosynthesis
1388348_at	BI278590	2	ELOVL5	ELOVL family member 5, elongation of long chain fatty acids	fatty acid elongase
1387183_at	J02844	2	Crot	carnitine octanoyltransferase	beta oxidation, transfer of fatty acyl groups between CoA and carnitine
1368426_at	NM_031987	2	Crot	carnitine octanoyltransferase	beta oxidation, transfer of fatty acyl groups between CoA and carnitine
1377921_at	AA875050	3	ETNK2	ethanolamine kinase 2	first step of phosphatidylethanolamine (PtdEtn) biosynthesis
1386960_at	NM_031589	3	Slc37a4, G6pt1	solute carrier family 37 member 4	transports glycerol-3-phosphate between cellular compartments
1367836_at	U88294	3	CPTI	carnitine palmitoyltransferase I, mitochondrial	fatty acid metabolism
1386946_at	NM_031559	3	Cpt1a	carnitine palmitoyltransferase 1 alpha, liver isoform	fatty acid metabolism
1371363_at	BI277042	4	Gpd1	glycerol-3-phosphate dehydrogenase 1 (soluble)	triglyceride synthesis
1370150_a_at	NM_012703	4	Thrsp, Lpgp, SPOT1	thyroid hormone responsive protein	activates genes encoding enzymes of fatty acid synthesis
1371400_at	AI169092	4	Thrsp, Lpgp, SPOT1	thyroid hormone responsive protein	activates genes encoding enzymes of fatty acid synthesis
1387852_at	NM_012703	4	Thrsp, Lpgp, SPOT1	Thyroid hormone responsive protein	activates genes encoding enzymes of fatty acid synthesis
1371012_at	AJ245707	4	Hpcl2	2-hydroxyphytanoyl-CoA lyase.	peroxisome, alpha-oxidation of 3-methyl-branched fatty acids
1368365_at	NM_031731	4	Aldh3a2	alcohol/aldehyde dehydrogenase family 3, subfamily A2	catalyzes oxidation of long-chain aldehydes derived from lipid metabolism
1390448_at	AA800699	4	Abhd13	abhydrolase domain containing 13	triglyceride storage
1386927_at	NM_012930	4	Cpt2	carnitine palmitoyltransferase 2 (Cpt2)	fatty acid metabolism
1372318_at	AI235528	5	ELOVL6	ELOVL family member 6, elongation of long chain fatty acids	fatty acid synthesis
1388108_at	BE116152	5	ELO2	fatty acid elongase 2	fatty acid synthesis
1369560_at	NM_022215	5	Gpd3	glycerol 3-phosphate dehydrogenase.	lipid and carrbohydrate metabolism
Transcription Regulation					
1370510_a_at	AB012600	1	BMAL1b, Arntl	aryl hydrocarbon receptor nuclear translocator-like	circadian transcription factor
1374753_at	AI105113	1	PAPD4	PAP associated domain containing 4	DNA binding, transferase activity
1370381_at	U61729	1	PNRC1, FBXO11	proline-rich nuclear receptor coactivator 1, F-box protein 11	nuclear, type II protein arginine methyltransferase
1398362_at	AI011448	1	NOTCH2	Transreg	notch homolog 2 (Drosophila)
1370928_at	BI284739	2	Litaf, RFX4	regulatory factor X, 4 (influences HLA class II expression)	winged-helix transcription factor
1373015_at	BI280348	2	Rnf11	ring finger protein 11	modulator of growth factor receptor signalling and transcription
1370975_at	AI172079	2	JMJD1A	jumonji domain containing 1A	STAT3 signaling, transcription
1367771_at	NM_031345	4	Gilz	glucocorticoid-induced leucine zipper	glucocorticoid-induced leucine zipper that inhibits NF-B activity
1371524_at	AI009608	4	Gtl3	trap locus 3, transcription factor IIB-like	transcription initiation in eukaryotes is mediated by the TATA-binding protein

Probe ID	Accession No.	Cluster	Symbol	Gene Name	Gene Function
1369270_at	NM_052980	4	Nr1i2	nuclear receptor subfamily 1, group I, member 2	pregnane X receptor (PXR) activates cytochrome P450-3A, xenobiotic and drug metabolism
1372320_at	BE103894	4	Msl31	male-specific lethal-3 homolog 1	chromatin remodeling and transcriptional regulation
1377042_at	BI288196	4	PCGF5,	polycomb group ring finger 5	chromatin remodeling
1374709_at	AI406795	4	HLF, PAR bZIP	hepatic leukemia factor	proline and acidic amino acid-rich basic leucine zipper transcription factor family (circadian)
1367541_at	BE113965	4	METTL5	methyltransferase like 5	DNA methylation
1373472_at	AI177008	5	Actr6	ARP6 actin-related protein 6 homolog(Actr6)	role in heterochromatin formation, nuclear
1370062_at	NM_080902	5	Hig1	HIG1 domain family, member 1A, Hypoxia-inducible gene 1	protects cells from apoptosis
1389412_at	AA800693	5	ZNF306	zinc finger protein 306	transcriptional regulation
1368303_at	NM_031678	5	Per2	period homolog 2 (Drosophila)	regulation of transcription, DNA-dependent; rhythmic behavior
1389420_at	BI279446	5	Stap2	signal-transducing adaptor protein-2	signal-transducing adaptor molecule, links several tyrosine kinases and STAT3
1371873_at	AA850735	5	ANP32E, Cpd1	acidic (leucine-rich) nuclear phosphoprotein 32 family, member E	nucleo-cytoplasmic shutteling phosphoprotein, chromatin remodeling
Bile Acid/Cholesterol					
1368336_at	NM_017126	1	Fdx1	ferredoxin 1.	steroid, vitamin D, and bile acid metabolism (mitochondrial)
1372755_at	AI102073	1	Mal2	T-cell differentiation protein 2, MAL PROTEOLIPID PROTEIN 2	basolateral-to-apical transcytosis
1387470_at	NM_031699	1	Cldn1	claudin 1	Ca(2+)-independent cell adhesion activity
1375933_at	BM392116	1	Cldn2	claudin 2	Ca(2+)-independent cell adhesion activity
1368769_at	NM_031760	2	Abcb11	ABC transport protein, sub-family B, member 11	major canalicular bile salt export pump
1374531_at	AA926305	2	Slc6a6	solute carrier family 6 (taurine), member 6	taurine is involved in bile acid conjugation
1368778_at	NM_017206	2	Slc6a6	solute carrier family 6 (taurine), member 6	taurine is involved in bile acid conjugation
1370940_at	BG378746	2	Tjp2	tight junction protein 2 (zona occludens 2)	bile acid transport and circulation
1375852_at	BM390399	4	Hmgcr	3-hydroxy-3-methylglutaryl-Coenzyme A reductase	rate-limiting step in cholesterol biosynthesis
1387848_at	NM_013134	4	Hmgcr	3-hydroxy-3-methylglutaryl-Coenzyme A reductase	rate-limiting step in cholesterol biosynthesis
1387017_at	NM_017136	4	Sqle	squalene epoxidase	cholesterol biosynthesis, catalyzes the first oxygenation step in sterol biosynthesis
1368275_at	NM_080886	4	Sc4mol	sterol-C4-methyl oxidase-like	cholesterol biosynthesis
1388872_at	BI290053	4	Idi1	isopentenyl-diphosphate delta isomerase	isoprenoid biosynthetic pathway (peroxisomal)
1368878_at	NM_053539	4	Idi1	isopentenyl-diphosphate delta isomerase	isoprenoid biosynthetic pathway (peroxisomal)
1374251_at	AA893192	4	Kir4.2, KCNJ15	potassium inwardly-rectifying channel, subfamily J, member 15	maintains charge balance during bile secretion
1368458_at	NM_012942	4	Cyp7a1	cytochrome P450 (cholesterol hydroxylase 7 alpha)	catalyzes the first step in bile acid synthesis
Cytoskeleton					
1375216_at	AA850909	1	Pvrl2	poliovirus receptor-related 2	cell surface protein
1389681_at	BI296388	2	Pvrl2	poliovirus receptor-related 2	cell surface protein
1371969_at	BI291848	2	CALD1	caldesmon 1	cytoskeletal remodeling
1376038_at	AI411054	2	CDC42	cell division cycle 42 (GTP binding protein, 25kDa)	delivery of newly synthesized proteins/ lipids to plasma membrane
1376572_a_at	AI045848	2	SVIL	Supervillin	link between actin cytoskeleton and membrane

Probe ID	Accession No.	Cluster	Symbol	Gene Name	Gene Function
1388566_at	AI102215	2	Lasp1	LIM and SH3 protein 1	regulation of dynamic actin-based, cytoskeletal activities
1375775_at	BI296701	2	ODF3	outer dense fiber of sperm tails 3	component of sperm flagella outer dense fibers
1388422_at	BI275904	2	Lims2	LIM and senescent cell antigen like domains 2	adhesion sites between cells and extracellular matrix (ECM)
1375941_at	BI292120	3	Baiap2l1	BAI1-associated protein 2-like 1	cytoskeletal regulation and cellular organization
1387856_at	BI274457	4	Cnn3	calponin 3, acidic	cytoskeleton
1388874_at	BE113032	4	Mtss1	metastasis suppressor 1	regulator of cytoskeletal dynamics, interacts with ATP-actin monomers
1368068_a_at	NM_130740	4	Pacsin2	protein kinase C and casein kinase substrate 2	organization of actin cytoskeleton and regulation of vesicular traffic
1389639_at	BF283302	4	PCDH1	protocadherin 1 (cadherin-like 1)	mediate calcium-dependent cell-cell adhesion
1387793_at	NM_021594	5	Slc9a3r1	solute carrier family 9 (sodium/hydrogen exchanger) isoform 3 regulator 1	actin cytoskeleton reorganization requires the activation of a sodium/hydrogen exchanger
1399082_at	AI176581	5	Tmem33	transmembrane protein 33	multipass membrane protein
Signaling					
1399005_at	BG673380	1	Ppp2r5a	protein phosphatase 2, regulatory subunit B	signaling
1368036_at	M60103	2	Ptprf	protein tyrosine phosphatase, receptor type, F	signaling, insulin
1373864_at	BM388810	2	MAP3K4	mitogen-activated protein kinase kinase kinase kinase 4	mediator of environmental stress, activates CSBP2 MAPK pathway
1398273_at	NM_053599	2	Efna1, B61	ephrin A1	receptor tyrosine kinase
1372844_at	AW531877	2	Efna1, B61	ephrin A1	receptor tyrosine kinase
1389169_at	AA944158	2	Pgrmc2	progesterone receptor membrane component 2	receptor
1388531_at	BF283382	2	Pgrmc2	progesterone receptor membrane component 2	receptor
1388659_at	BI295783	2	Carhsp1	calcium regulated heat stable protein 1	IGF-I signaling kinase substrate
1373777_at	BF391820	3	RGS16	regulator of G-protein signaling 16	inhibits G protein-coupled mitogenic signal transduction and activation (MAPK) cascade
1371543_at	AI170047	4	Mtmr2	myotubularin related protein 2	protein-tyrosine phosphatase, non-receptor
1373842_at	BM390718	4	N-WASP	Neural Wiskott-Aldrich syndrome protein	transmission of signals from tyrosine kinase receptors and small GTPases to cytoskeleton
1373277_at	BG373457	5	Tm2d3	TM2 domain containing 3	G protein-coupled receptor
1373162_at	AI600085	5	Tmem41a	transmembrane protein 41a	multipass membrane protein
1372752_at	BF282632	5	Tspan4	tetraspanin 4	complexes with integrins and other cell-surface proteins
Small Molecule Metabolism					
1377375_at	AA944898	1	Aass	aminoadipate-semialdehyde synthase	lysine-degradation
1375856_at	AI102258	1	ABAT	4-aminobutyrate aminotransferase	catabolism of gamma-aminobutyric acid (GABA)
1375215_x_at	BE109558	1	Pgpep1	pyroglutamyl-peptidase I	drug and TRH metabolizing enzyme
1398282_at	NM_053902	2	Kynu	kynureninase (L-kynurenine hydrolase)	tryptophan-nicotinic acid pathway decreased formation of nicotinic acid
1387156_at	NM_024391	3	Hsd17b2	17-beta hydroxysteroid dehydrogenase type 2	catalyzes interconversion of testosterone and androstenedione, as well as estradiol & estrone
1389430_at	AI176172	4	Hsd17b7	hydroxysteroid (17-beta) dehydrogenase 7	oxidizes or reduces estrogens and androgens
1387233_at	NM_017235	4	Hsd17b7	hydroxysteroid (17-beta) dehydrogenase 7	oxidizes or reduces estrogens and androgens
1387109_at	NM_031576	4	Por	NADPH-cytochrome P-450 oxidoreductase	donates electrons to all microsomal P450 enzymes

Probe ID	Accession No.	Cluster	Symbol	Gene Name	Gene Function
1371031_at	AI454484	4	Mat1a	methionine adenosyltransferase I, ALPHA	catalyzes formation of adenosylmethionine from methionine and ATP
1368213_at	AI407454	4	Por	P450 (cytochrome) oxidoreductase	donates electrons to all microsomal P450 enzymes
1387659_at	AF245172	5	Gda	guanine deaminase; EC 3.5.4.3	catalyzes hydrolytic deamination of guanine
1387336_at	NM_022635	5	Cml4	N-acetyltransferase Camello 4	drug metabolism in liver
Carbohydrate/Glucose Metabolism					
1388318_at	BI279760	1	Pgk1	Phosphoglycerate kinase 1	glycolysis
1371251_at	L05541	2	GALT	galactose-1-phosphate uridyltransferase	interconversion of galactose-1-phosphate and glucose-1-phosphate
1390172_at	AI409946	2	Dhtkd1	dehydrogenase E1 and transketolase domain containing 1	oxoglutarate dehydrogenase (succinyl-transferring) activity
1387203_at	NM_013120	2	Gckr	glucokinase regulatory protein	inhibits glucokinase
1387361_s_at	NM_053291	2	Pgk1	Phosphoglycerate kinase 1	glycolysis
1387228_at	NM_012879	3	Slc2a2, Glut2	solute carrier family 2 A2	low-affinity glucose transporter, type 2
1393516_at	AA892335	3	Slc16a12	solute carrier family 16, member 12	monocarboxylic acid transporters: lactate, pyruvate
1390530_at	AI169239	3	Slc16a12	solute carrier family 16, member 12	monocarboxylic acid transporters
1369467_a_at	NM_012621	4	Pfkfb1	6-Phosphofructo-2-kinase/fructose-2,6-bisphosphatase 1	glycolysis
1368460_at	NM_031741	4	Slc2a5	solute carrier family 2, member 5	facilitated glucose transporter
1372602_at	BI295979	4	SBP	genethonin 1	starch binding protein
1370299_at	M10149	5	Aldob	aldolase B; liver	glycolysis
1368328_at	NM_013089	5	Gys2	glycogen synthase 2 (liver).	glucose storage
Mitochondrial					
1376427_a_at	AI029729	1	Gldc	glycine decarboxylase	mitochondrial, glycine cleavage system
1398891_at	AI103129	1	Mrpl15	mitochondrial ribosomal protein L15	mitochondrial
1374765_at	BI288055	2	Bdh1	3-hydroxybutyrate dehydrogenase, type 1	mitochondrial membrane, specific requirement for phosphatidylcholine
1371519_at	AA851258	2	Etfdh	electron-transferring-flavoprotein dehydrogenase	inner mitochondrial membrane
1372715_at	AA819349	3	SLC25A1	liver tricarboxylate carrier, mitochondrial	mitochondrial, solute carrier
1373282_at	AI406494	3	SLC25A33	mitochondrial carrier protein MGC4399	mitochondrial inner membrane
1373383_at	AA848807	4	Mterfd1	MTERF domain containing 1	mitochondrial transcription termination factor
1367982_at	NM_024484	4	Alas1	aminolevulinic acid synthase 1	mitochondrial, rate-limiting enzyme in heme biosynthesis
1398349_at	AI411497	5	Ak2	adenylate kinase 2	mitochondrial, ATP:AMP phosphotransferase
1367670_at	NM_017005	5	Fh1	fumarate hydratase	mitochondrial, Krebs cycle, fumarate to malate
1399058_at	BI288800	5	Mrpl18	mitochondrial ribosomal protein L18	mitochondrial
1371634_at	BE107851	5	TMEM126A	transmembrane protein 126A	mitochondrial
Immune					
1373515_at	BI275737	1	MAC2	galectin-5 (RL-18)	macrophage galactose-specific lectin
1372004_at	AI102065	1	HEBP1	heme binding protein 1	chemoattractant for dendritic cells and monocytes
1367850_at	NM_053843	1	Fcgr3	Fc receptor, IgG, low affinity III	neutrophil-specific antigen
1372056_at	AI406687	2	Cmtm6	CKLF-like MARVEL transmembrane domain containing 6	chemokine-like factor superfamily member 6
1386987_at	NM_017020	3	Il6r	interleukin 6 receptor.	cell surface receptor linked signal transduction
1383013_at	AI045857	3	Klf13	kruppel-like factor 13	transcription F dominant transactivator of RANTES in T-cells
1380905_at	AA893260	3	IL32	interleukin 32	a cytokine and inducer of TNFalpha
1373986_at	AI410107	3	TNFSF11	tumor necrosis factor superfamily, member 11	ligand for TNF receptor, RANKL receptor, activator of NF-kappa-B ligand

Probe ID	Accession No.	Cluster	Symbol	Gene Name	Gene Function
1388102_at	U66322	4	DIG-1	dithiolethione-inducible gene-1.	inhibits pro-inflammatory actions of LTB4
1382255_at	BE110785	4	PBEF1	visfatin, pre-B-cell colony-enhancing factor 1	type II phosphoribosyltransferase enzyme involved in NAD biosynthesis
1371770_at	AW434268	5	Ke2	MHC class II region expressed gene KE2	centromeric end of major histocompatibility complex
Protein Degradation					
1368184_at	NM_130430	1	Psmd9	proteasome (prosome, macropain) 26S subunit, non-ATPase, 9	covalent attachment of ubiquitin
1389480_at	AI598462	4	Rwdd4a	RWD domain containing 4A	ubiquitin protein ligase activity
1372115_at	AI408477	4	UBR2	ubiquitin protein ligase E3 component n-recognin 2	recognize substrate's destabilization signal, proteolysis
1375549_at	AI407719	4	Usp2	ubiquitin specific peptidase 2	disassembly of polyubiquitin chains
1387703_a_at	AF106659	4	Usp2	ubiquitin-specific, cysteine protease	disassembly of polyubiquitin chains
1376849_at	BM384872	5	Usp48	ubiquitin specific protease 48	protein ubiquitination
Other					
1398950_at	BI275914	1	Scel	sciellin	assembly/regulation of proteins in cornified envelope
1398902_at	BF282978	1	EST	mKIAA0664 protein	unknown function
1390042_at	AI071166	1	EST	Unknown	unknown function
1373312_at	BI295064	1	Pnkd	paroxysmal nonkinesiogenic dyskinesia	stress, hydroxyacylglutathione hydrolase, detoxify methylglyoxal
1367838_at	NM_017074	1	Cth	CTL target antigen (Cth)	hepatic synthesis of glutathione
1389156_at	BM384589	2	LOC498606	hypothetical protein LOC498606	unknown function
1376709_at	BM388442	2	Slc39a8	solute carrier family 39 (metal ion transporter), member 8	zinc transporter
1387038_at	NM_053425	3	Ccs	copper chaperone for superoxide dismutase	copper chaperone
1376868_at	BM389293	3	Cobll1	Cobl-like 1(Cordon-bleu)	unknown function
1389717_at	AI171467	4	EST	KIAA0157	unknown function
1389561_at	BE110624	4	EST	Unknown	unknown function
1389256_at	BG381256	4	EST	Unknown	unknown function
1373870_at	BE110630	4	FAM98A	family with sequence similarity 98, member A	unknown function
1371147_at	X69834	4	SERPINA3	serine protease inhibitor 2.4.	plasma protein
1369976_at	NM_053319	5	Pin	dynein, cytoplasmic, light chain 1	effects nitric oxide synthase activity
1392928_at	AA891693	5	PXMP3	peroxisomal membrane protein 3, 35kDa (Zellweger syndrome)	peroxisome assembly
1388534_at	AA851369	5	SLC31A1	solute carrier family 31, member 1	high-affinity copper uptake
1388325_at	BF281358	5	Atp6v1d	ATPase, H+ transporting, V1 subunit D	vacuolar-type proton pump ATPase transport
1371564_at	AI169159	5	Atp6v1e1	ATPase, H+ transporting, V1 subunit E isoform 1	vacuolar-type proton pump ATPase transport
1382048_at	BI289589	5	MYO1D	myosin ID	molecular motors, intracellular movements
1380547_at	BI288519	5	CLCN3	chloride channel 3	voltage-gated chloride channel
1371976_at	AI102758	5	EST	Unknown	unknown function
1371916_at	AI409380	5	SEPX1	selenoprotein X, 1	scavenging of ROS, oxudative stress
1371763_at	BI274533	5	EST	Unknown	unknown function
1368230_a_at	U95161	5	LOC56769	nuclear protein E3-3	unknown function